

**MIMICKING THE TUMOR MICROENVIRONMENT IN  
LAB-ON-A-CHIP DEVICES**

**A Thesis Submitted to  
The Graduate School of Engineering and Sciences of  
İzmir Institute of Technology  
in Partial Fulfillment of the Requirements for the Degree of**

**MASTER OF SCIENCE**

**in Biotechnology and Bioengineering**

**by  
Müge BİLGİN**

**July 2019  
İZMİR**

We approve the thesis of Müge BİLGEN

**Examining Committee Members:**



**Prof. Dr. Devrim PESEN OKVUR**

Department of Molecular Biology and Genetics, Izmir Institute of Technology



**Asst. Prof. Dr. Hüseyin Cumhuri TEKİN**

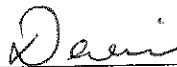
Department of Bioengineering, Izmir Institute of Technology



**Asst. Prof. Dr. Yavuz OKTAY**

Department of Medical Biology, Dokuz Eylül University

16 July 2019



**Prof. Dr. Devrim PESEN OKVUR**

Supervisor, Department of Molecular Biology and Genetics, Izmir Institute of Technology



**Asst. Prof. Dr. Nur Başak SÜRMEİ**

Co-Supervisor, Department of Bioengineering, Izmir Institute of Technology



**Assoc. Prof. Dr. Engin ÖZÇİVİCİ**

Head of the Department of Biotechnology and Bioengineering, Izmir Institute of Technology

**Prof. Dr. Aysun SOFUOĞLU**

Dean of the Graduated School of Engineering and Sciences

## ACKNOWLEDGMENTS

I would like to express my deepest appreciation and thanks to supervisor Prof. Dr. Devrim PESEN OKVUR for her patience, encouragement, understanding and instructive guidance throughout this study.

I would like to thank also the members of my thesis defense committee Assist. Prof. Dr. H. Cumhuri TEKİN and Assist. Prof. Dr. Yavuz OKTAY for helpful comments and giving suggestions. I also would like to thank TUBITAK for finance this thesis with 1001 project (115Z428).

I would like to express my deepest appreciation and thanks to my friends and colleagues of Controlled *in vitro* Microenvironments (CivM) Laboratory for their support Gizem BATI AYAZ, Begüm GÖKÇE, Aslı KISIM, İsmail TAHMAZ, Derya USTA, Osman Halil SUBAY, Ali YETGİN and Ali CAN. In addition, I also appreciate to lovely alumni Sevgi ÖNAL, Deniz KANKALE, Nurullah SATI and Yeşim ŞİRİN.

I would like to thank also Burcu FIRATLIGIL YILDIRIR, Ceren TABAK BURU, Özge KARADAŞ and Öznur BAŞKAN as my colleague and any other support.

I would like to thank also my lovely friends İdil YILMAZ, Görkem KÜÇÜK, Eda EŞİT, Ece Çalışkan, Meltem KARACA, Özge Sevin KESKİN, Yasemin BİLGİ, Fikrican DİLEK, Elif GÜREL, Aslı ADAK, Revna ERGÜN, Zeynep Güngören and Atıl Buğrahan Arslan.

Finally, I would like to explain my special appreciation and endless thanks to my lovely family Neşe KOCASARI, Ahmet Melih BİLGİN, Özlem BİLGİN, Simge İrem BİLGİN, Deniz NART, Ahmet NART and Batu NART for their infinite support all over my life.

# ABSTRACT

## MIMICKING THE TUMOR MICROENVIRONMENT IN LAB-ON-A-CHIP DEVICES

Breast cancer is one of the cancers with the highest incidence and mortality rates in women in the world. The leading cause of death for cancer patients is tumor metastasis. Cancer cells can extravasate the blood vessel, go through the distant organs and form the metastasis. Tumor microenvironment comprises of cancer and normal cells, extracellular matrix, soluble biological and chemical factors. Biochemical aspects of the interactions of cancer cells with the constituents of the microenvironment are widely studied whereas biophysical studies are at limited numbers. There is increasing evidence that extracellular matrix can change the mechanics and function of cancer and stroma cells. It has been observed that cancer cells show different responses to soft and stiff tissues they are in direct contact with than normal cells. New cell culture setups should be developed to better understand the interactions of cancer cells with their microenvironment.

To develop a three dimensional (3D) in vitro model will allow the study of stiffness which is one of the mechanical features of extracellular matrix features first, 3D (dimensional) Controlled in vitro Microenvironments (CivMs) that mimic a blood vessel and its neighboring tissue in vivo will be fabricated using UV lithography. Monolayer which was formed by endothelial cells play a role in pathophysiological processes, so it shows a barrier role between both blood and tissues. To form a blood vessel bEnd.3 cell line was used. Collagen which is the most abundant protein in connective tissues were used to mimic extracellular matrix. pH value of collagen was changed and represented two different stiffness value.

Here, the in vitro model we define as controlled in vitro microenvironments (CivM) is a lab-on-a-chip (LOC) application. In this microenvironment; MDA-MB-231 cells which are known to be invasive and MCF10A which is normal mammary epithelial cells were used as control. LOC devices were used to investigate cancer cell extravasation which is the prominent step of metastasis and extracellular matrix relation.

## ÖZET

### YONGA-ÜSTÜ-LABORATUVAR AYGITLARINDA TÜMÖR MİKROÇEVRESİNİN TAKLİT EDİLMESİ

Meme kanseri tüm dünyada kadınlarda en sık rastlanan ve aynı zaman ölüm oranı yüksek olan kanser çeşididir. Kanser hastaları için ilk sırada gelen ölüm sebebi, tümör metastazıdır. Kanser hücreleri damardan çıkarak (ekstravazasyon) birincil organdan farklı organlara giderek metastaz yapmaktadırlar. Tümör mikro çevresi, sağlıklı ve kanserli hücreleri, hücre dışı matriksi, çözünür halde biyolojik ve faktörlerini ve kimyasal etkenleri içerir. Kanser hücrelerinin mikro çevre bileşenleri ile etkileşimlerinin biyokimyasal yönleri yaygın olarak incelenmektedir; fakat biyofiziksel çalışmalar sınırlı sayıdadır. Hücre dışı matriksin kanser ve destek doku hücrelerinin mekaniğini ve işlevlerini değiştirebildiğine dair kanıtlar artmaktadır. Kanser hücrelerinin doğrudan temas halinde oldukları sert ve yumuşak dokulara normal hücrelerden farklı tepkiler verebildikleri de görülmüştür. Kanser hücrelerinin mikro çevreleri ile olan etkileşimlerinin daha iyi anlaşılabilmesi için yeni hücre kültürü düzenekleri oluşturulması gerekmektedir.

Ekstravazasyon ile hücre dışı matriksin mekaniksel özelliklerinden biri olan sertliğin incelenmesini sağlayacak üç boyutlu bir in vitro modelin geliştirilmesi için öncelikle UV litografi kullanarak canlıda bir kan damarını ve komşu olduğu dokuyu taklit eden 3B (üç boyutlu) kontrollü in vitro mikro çevreler oluşturulmuştur. Kan damarı dokularla kan arasında bariyer olarak görev alır. Kan damarı oluşturmak için bEnd.3 endotel hücre hattı kullanılmıştır. Bağ dokusunda yüksek miktarda bulunan kolajen hücre dışı matriksi taklit etmek için kullanılmış ve pH değerlerine göre farklı sertlik derecelerine göre ikiye ayrılmıştır.

Burada kontrollü in vitro mikro çevre olarak tanımladığımız in vitro model, yonga-üstü-laboratuvar uygulamasıdır. Bu mikro çevrelerde invaziv oldukları bilinen MDA-MB-231 hücreler ile kontrol olarak normal meme epitel hücreleri olan MCF10A kullanılmıştır. Bu çalışmada metastazın önemli basamaklarından olan ekstravazyonun hücre dışı matriksin sertliği ile olan ilişkisi incelenmiştir.

*To my family...*

# TABLE OF CONTENTS

LIST OF FIGURES .....	ix
LIST OF ABBREVIATIONS .....	xii
CHAPTER 1 INTRODUCTION .....	1
1.1. Cancer .....	1
1.2. Breast Cancer .....	2
1.3. Metastasis .....	3
1.4. Extra Cellular Matrix .....	4
1.5. Stiffness.....	5
1.6. Lab-on-a-chip.....	9
1.7. Aim of the Study .....	11
CHAPTER 2 MATERIALS AND METHODS .....	12
2.1. Cell Culture .....	12
2.1.1. Medium Preparation of bEnd.3 Cell Line .....	12
2.1.2. Medium Preparation of MDA-MB-231 Cell Line.....	12
2.1.3. Medium Preparation of MCF-10A Cell Line .....	13
2.1.4. Cell Passage .....	13
2.1.5. Cell Thawing .....	14
2.1.6. Cell Freezing .....	15
2.1.7. Cell Tracking .....	15
2.2. LOC Device Fabrication .....	15
2.2.1. UV – Lithography.....	16
2.2.2. Polydimethylsiloxane (PDMS) Molding .....	18
2.2.3. PDMS Punching and Cleaning .....	18
2.2.4. PDMS Bonding.....	19
2.2.5. Channel Height Measurement .....	19

2.3. LOC Device Coating.....	20
2.4. Dextran Preparation .....	20
2.5. Gel Preparation.....	21
2.5.1. Matrigel and Collagen Preparation.....	21
2.5.2. Collagen pH Measurement .....	21
2.6. Endothelial Monolayer Formation .....	22
2.7. Endothelial Monolayer Integrity .....	22
2.8. Perfusion .....	23
2.9. Extravasation Quantification.....	24
2.10. Distance of Extravasated Cell Quantification .....	26
CHAPTER 3 RESULT AND DISCUSSION .....	28
3.1. LOC Device Fabrication with using UV Lithography Method .....	28
3.2. Determination of Collagen pH.....	29
3.3. Coating Optimization of Lab-on-a-chip Device for the Formation of Endothelial Monolayer .....	32
3.4. Dextran used for Endothelial Monolayer.....	35
3.5. Endothelial Monolayer Formation .....	36
3.6. Determination of Permeability Differences .....	38
3.7. Extravasated Cell Analysis .....	40
3.8. Distance Migrated by Extravasated Cell.....	43
CHAPTER 4 CONCLUSION .....	46
REFERENCES .....	48



# LIST OF FIGURES

<u>Figure</u>	<u>Page</u>
Figure 1.1. The six hallmarks of cancer.....	1
Figure 1.2. The metastatic process overviews. ....	4
Figure 1.3. Extracellular Matrix and metastasis process relation. ....	5
Figure 1.4. Stiffness value of some materials. ....	7
Figure 1.5. Stiffness value of some body organs and tissues. ....	7
Figure 1.6. Adjusted different pH value of collagen and their effects on migration. ....	8
Figure 1.7. Relation between pH of collagen solution and collagen stiffness in relaxation modulus. ....	9
Figure 1.8. Comparison of in vitro and in vivo models. ....	10
Figure 2.1. The fabrication process of UV Lithography.....	17
Figure 2.2. Image represent height difference of LOC devices according to angle. ....	24
Figure 2.3. Shear stress and angle calculation according to height differences and flow rate values.....	24
Figure 2.3. a) Yellow circle shows extravasated cell in vertical view of endothelial monolayer. b) Zoom in extravasated cell in horizontal view of endothelial monolayer. ....	25
Figure 2.4. Cells in endothelial monolayer represents in flow channel. a) vertical view of endothelial monolayer. b) horizontal view of endothelial monolayer. ....	25
Figure 2.5. a) Yellow circle shows associated cell in vertical view of endothelial monolayer. b) Zoom in associated cell in horizontal view of endothelial monolayer. ....	26
Figure 2.6. Representative image shows that distance of extravasated cell from the endothelial monolayer. ....	26
Figure 2.7. Experimental flow scheme. ....	27
Figure 3.1. a) Image of SU-8 mold (wafer). b) Image of PDMS of Lab-on-a-chip device. c) Design of mask. d) Image of PDMS LOC device after permanent bonding onto glass slide by UV/ozone treatment. ....	28
Figure 3.2. The tested amounts which are between 1 and 7 $\mu$ l were shown in table both in $\mu$ l and $\mu$ mole of NaOH values. At the same time, graphics were represented the exact pH value corresponding to the $\mu$ mole value. ....	29
Figure 3.3. The tested amounts which are 7.14 – 21.42 – 42.84 – 50 $\mu$ l were shown in table both in $\mu$ l and $\mu$ mole of NaOH values. ....	30

<u>Figure</u>	<u>Page</u>
Figure 3.4. The tested amounts which are 20, 25 and 30 $\mu\text{l}$ were shown in table both in $\mu\text{l}$ and $\mu\text{mole}$ of NaOH values. At the same time, graphics were represented the exact pH value corresponding to the micromole value. ....	30
Figure 3.5. The tested amounts which are 2, 10, 20, 25 and 50 $\mu\text{l}$ at 0.3 M were shown in table both in $\mu\text{l}$ and $\mu\text{mole}$ of NaOH values. At the same time, graphics were represented the exact pH value corresponding to the $\mu\text{mole}$ value. ....	31
Figure 3.6. Measurement of Collagen pH according to different NaOH amount. a-c) 0.1 M NaOH, d) 0.3 M NaOH.....	31
Figure 3.7. All tested amounts graphics were represented the exact pH value corresponding to the micromole value. ....	32
Figure 3.8. 3D microscope images of first day of 2% APTES-FN (0.0125 mg/ml) and 2% APTES-PLL (0.1 mg/ml) coated LOC devices with endothelial cells dissolved in dextran media. Images were taken with confocal microscope. a-b) Different positions of APTES – FN coated LOC devices. c-d) Different positions of PLL – FN coated LOC devices. ....	33
Figure 3.9. 3D microscope images were taken by confocal microscope of after bEnd.3 endothelial cells loading at a concentration $7.5 \times 10^6 / \text{ml}$ with 2% APTES - COL ( $5 \mu\text{g}/\text{ml}$ ) coated LOC device. a) first day, b) second day, c) third day.....	34
Figure 3.10.3D microscope images were taken by confocal microscope of after bEnd.3 endothelial cells loading at a concentration $7.5 \times 10^6 / \text{ml}$ with 2% APTES – LAM (0.0125 mg/ml) coated LOC device. a) first day, b) second day, c) third day.....	34
Figure 3.11.3D microscope images were taken by confocal microscope of after bEnd.3 endothelial cells loading at a concentration $7.5 \times 10^6 / \text{ml}$ with 2% APTES – FN (0.0125 mg/ml) coated LOC device. a) first day, b) second day, c) third day. ....	34
Figure 3.12.3D microscope images of after bEnd.3 endothelial cells dissolved in dextran media and own media respectively loading at a concentration $8.7 \times 10^6 / \text{ml}$ with LOC device. a - c) Horizontal side view. b - d) Vertical side view. ....	35
Figure 3.13.3D microscope images of after bEnd.3 endothelial cells dissolved in dextran media loading at a concentration $22 \times 10^4 / \text{ml}$ with LOC device. a) Horizontal side view of green tracker labeled bEnd.3 cells.b) Horizontal side view of bright field. ....	36
Figure 3.14.3D microscope images were taken by confocal microscope of after bEnd.3 endothelial cells loading at a concentration $5.8 \times 10^6 / \text{ml}$ with 2% APTES – Laminin (0.0125 mg/ml) coated LOC device. ....	37

<u>Figure</u>	<u>Page</u>
Figure 3.15. In matrix channel stiff collagen (high pH) was loaded. Then, 2% APTES – Laminin (0.0125 mg/ml) coated LOC device were loaded with bEnd.3 endothelial cells which was at a concentration $5.2 \times 10^6$ / ml. ....	37
Figure 3.16. In matrix channel soft collagen (low pH) was loaded. Then 2% APTES – Laminin (0.0125 mg/ml) coated LOC device were loaded with bEnd.3 endothelial cells which was at a concentration $5.2 \times 10^6$ / ml. ....	38
Figure 3.17. After 70kDa dextran loaded in flow channel. a) Low pH value collagen; top side bEnd.3 cells (488) 0-30-60 min. bottom side dextran (555). b) High pH value collagen; top side bEnd.3 cells (488) 0-30-60 min. bottom side dextran. ....	39
Figure 3.18. As a result of pH dependent collagen stiffness increased, cell-cell junction between endothelial cells were disrupted. For this reason, permeability is increased in high pH value of collagen. ....	39
Figure 3.19. Extravasated cell number into matrix. Black line represents differences between MDA-MB-231 and MCF10A cells ( $p < 0.001$ ***), dashed lines represents differences between flow and static conditions of MDA-MB-231 cells in same matrix. ( $p < 0.05$ *) ....	41
Figure 3.20. Extravasated cells metric in endothelial monolayer. ( $p < 0.05$ *), ( $p < 0.001$ ***) ....	41
Figure 3.21. Associated cell number into matrix. Black line represents differences in MDA-MB-231 between soft and stiff matrix ( $p < 0.05$ *), dashed lines represents differences between MDA-MB-231 and MCF10A cells in soft matrix under static condition. ( $p < 0.05$ *) ....	42
Figure 3.22. Cells number in flow channel. ....	42
Figure 3.23. Distance of extravasated MDA-MB-231 cells both in stiff (high pH) and soft matrix (low pH) under flow and static condition. ( $p < 0.01$ **) ....	43
Figure 3.24. Distance of extravasated MCF10A cells both in stiff and soft matrix under flow and static condition. ( $p < 0.05$ *) ....	44
Figure 3.25. Comparison of distance of extravasated MDA-MB-231 and MCF10A cells in soft matrix under flow and static condition. ( $p < 0.001$ ***) ....	44
Figure 3.26. Comparison of distance of extravasated MDA-MB-231 and MCF10A cells in stiff matrix under flow and static condition. ( $p < 0.001$ ***) ....	45

## LIST OF ABBREVIATIONS

APTES	(3-Aminopropyl) triethoxysilane
COL	Collagen
ddH <sub>2</sub> O	Double distilled water
ECM	Extracellular Matrix
EtOH	Ethanol
FN	Fibronectin
LAM	Laminin
LOC	Lab-on-a-chip
NaOH	Sodium Hydroxide
PDMS	Polydimethylsiloxane
PLL	Poly-L-Lysine
UpH <sub>2</sub> O	Ultrapure water

# CHAPTER 1

## INTRODUCTION

### 1.1. Cancer

The main cause of global deaths is based on noncommunicable disease and cancer is one of them. In this era, it is expected that the most important obstacle to gaining the quality of life and the primary cause of death will be cancer disease in all around the world <sup>1</sup>. It is thought that the percentage of cancer prediction can increase that by the year 2020 in the world. The researches proposed that the total amount of recent cancer cases diagnosed annually can increase to fifteen million. Moreover, this disease cases may reach to twelve million deaths <sup>2</sup>. Cancer could be arising from any type of cells in our body. Fundamentally, cancer is the process of uncontrolled proliferation which is resulted in cell transformation. Both epigenetic and molecular changes that was occurred this period lead to cell development <sup>3</sup>. According to studies, six biological features of cancer cells which was obtained in their progression process had been discovered (Figure 1.1.) <sup>4</sup>. Because of revealing in DNA mutations, cancer cells go through limit zone of the growing tissue and repression of suppressor genes occurred. Thus, cells prevent themselves from apoptosis. It stimulates the formation of the vasculature under favor of metastasis capability <sup>5</sup>.

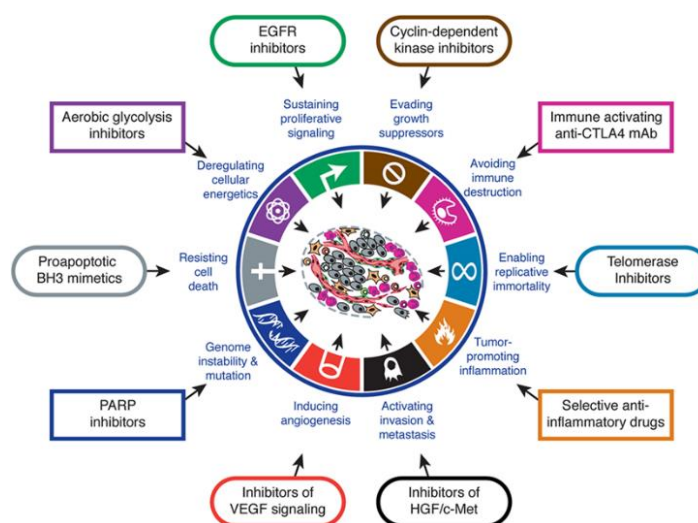


Figure 1.1. The six hallmarks of cancer (Source: Hanahan et al.<sup>6</sup>).

## 1.2. Breast Cancer

Breast cancer occurs as a result of the malignant tumor developing in the breast tissue. It is formed stromal and epithelial part of normal mammary glands which comprise of lobes and ducts. They are constitutionally ingrained in stroma. Breast tissue is responsible for production of milk and carrying out storage<sup>7,8</sup>. Breast cancer is one of the most common types of cancer among women in the world and has a high mortality rate<sup>9</sup>. It is stated that one out of every 37 women has died due to these cancer type and it corresponds to a rate of 2.7 percent<sup>10</sup>.

Although all the causes and mechanisms are not known exactly, both genetic and environmental factors affect to occurrence of breast cancer. Example of these factors include; alcohol and cigarette consumption, obesity, metabolic and hormonal factors, family history, early menstruation, feeding method and radiation exposure<sup>11</sup>. Breast cancer is a type of heterogeneous disease. Among the cancers in worldwide, breast cancer involves 12% part. Breast cancer is divided into two types; invasive and non-invasive. This distinction is determined by the ability of spread and the growth pattern. In non-invasive type; after proliferation cells remain in the same field where they originate. It is usually found in breast lobule or duct. In contrast, invasive type has a metastasize capability to distant organs and it also performs by invading basement membrane<sup>12</sup>. The incidence of breast cancer in women increases with age, moreover it is seen commonly in postmenopausal period women. In addition, diagnosis of breast cancer is doubled in women who has menopause period after the age 55<sup>13</sup>. Mostly breast cancer is seen in middle-aged women, in contrast this cancer type is rarely observed in men. Survival rate is higher in older-age women when compared to younger age women<sup>14</sup>. According to studies, breast cancer which has distinct biological and pathological properties shown different behaviors. For this reason, various treatment responses are required, and it should have applied distinct therapeutic strategies<sup>15</sup>. The breast cancer cells formed in primary region then it can spread secondary region by way of blood vessels to different distant organs. After dissemination, breast carcinoma is occurred metastases in different organs. Metastases often develop in more than one region in patients. The specific metastatic sites of breast cancer are liver, bone and lung<sup>16</sup>. According to study result, 2,088,849 new cases of breast cancer will be formed, and 626,679 breast cancer related death will be occurred worldwide at the end of 2018 all<sup>1</sup>.

### 1.3. Metastasis

Endothelial barrier has shown selective barrier function among the blood and blood vessel. When the endothelial barrier loss their function, various diseases arise as a result of this situation which includes cancer metastasis, pulmonary edema and atherosclerosis <sup>17</sup>. Cancer has six different hallmarks and metastasis is one of them. Malignant cancer is distinguished by cancer metastasis <sup>6</sup>. It causes 90% of deaths associated with cancers <sup>18</sup>. Cancer cells disseminate from primary site to distant organs in the body, this situation is called metastasis <sup>19</sup>. Metastatic tumors are formed in secondary site. For this reason, this is considered to be the main threat of cancer. Metastasis which has different steps is affected by various both cellular and molecular features of host organ <sup>20</sup>. Tumor development is also affected not only genetic and environmental properties but also structural features of tumor microenvironment <sup>21</sup>. The reason why we still do not understand the relationship between cancer and metastasis; transformation of physical stimulus, like cell-cell/ECM relation, to biochemical response in the tumor microenvironment is due to the poor understanding during tumor development <sup>22-24</sup>. Metastasis consist various steps (Figure 1.2.). Firstly, cancer cells separate from primary tumor then migration is occurred. They are intravasate to the vascular system with the help of capillaries. Cancer cells which are originated from primary tumor enter into blood stream, these cells entitled circulating tumor cells <sup>25</sup>. When the cancer cells are in the blood system, they have to pass over endothelial cell barrier. Then they spread out the tissue beneath, this step is also called extravasation <sup>26</sup>. Circulating tumor cells may spread through the circulation to distant sites. These cells could form secondary tumors in different tissues <sup>27</sup>. The most prominent step in development of cancer is extravasation because of the induce of seconder micro metastases in different organs <sup>28</sup>.

Paget's study showed that metastasis was not caused by chance occasions. In that study microenvironment of specific organs were selected by tumor cells and they developed specially in there. Tumor cells were represented "seed" and microenvironment was represented "soil". So, metastasis formed just when the proper seed was embedded in its appropriate soil <sup>29</sup>.

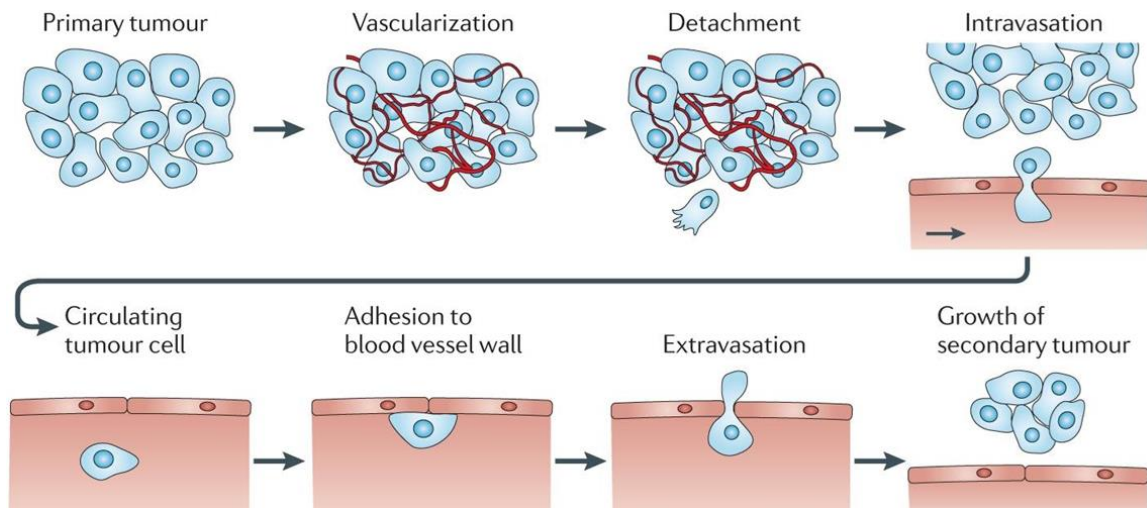


Figure 1.2. The metastatic process overviews (Source: Wirtz et al.<sup>30</sup>).

#### 1.4. Extra Cellular Matrix

Extracellular matrix is defined a kind of complicated network of macromolecules which has a various biochemical and mechanical feature <sup>31</sup>. The Extracellular matrix (ECM) is surrounding cells which is a type of cell-embedded network. ECM consists of mainly fibrous protein and proteoglycans. ECM imparts mainly structural support. Besides that, it shows both biochemical and mechanical properties which can provides to organize behaviors of cells <sup>32</sup>. The complex organisms are made up of tissues that are formed by embedding cells in the extracellular matrix <sup>33</sup>. ECM has many different functions. It shows structural features for function of tissue and mechanic integration. In addition, it provides to regulate amount of growth factors and cytokines and preserves the pH or hydration of the microenvironment <sup>34, 35</sup>. As a result of interactions among endothelial cells and ECM, the dynamically opening and closing of endothelial cell-cell junctions is affected. This situation partially controls the permeability of endothelial <sup>36</sup>. According to recently researches, cell integrin binds to ECM and send cellular response to soluble factors and is assigned an important responsibility in altering cellular behavior in culture as well. Therefore, that thing is understood that relationship between cells and their local environments reaches far beyond native interactions <sup>37, 38</sup>. According to one study in 2011 <sup>6</sup>, which was belonged to Hanahan and Weinberg, re-reviewed the hallmarks of cancer (Figure 1.3.). Two novel properties were added these hallmarks; abolish of



immune destruction and dysregulation of cellular metabolism. Evidence shows that many of cellular responses which indicates the hallmarks of cancer are regulated by ECM. Because of this reason all features of ECM should take in consideration during the investigate behavioral features of tumor and therapeutic response <sup>39</sup>. Undoubtedly, distinguishing ‘ECM signature’ is related to metastasis capacity and specific site of distant tissue <sup>40</sup>. Model system which mimics different tissue sites is created from basic to complex by engineers because of enhance the understanding of genetically details. These model systems consist of mainly healthy cells which is found in mimicking tissue, viscoelastic properties of ECM, tissue dimensionality and protein composition of ECM. In tissue mimicking, hydrogels are mostly use because of some properties, such as ability to repeat some properties of structure of 3D and hold a physiologically water content <sup>41</sup>.

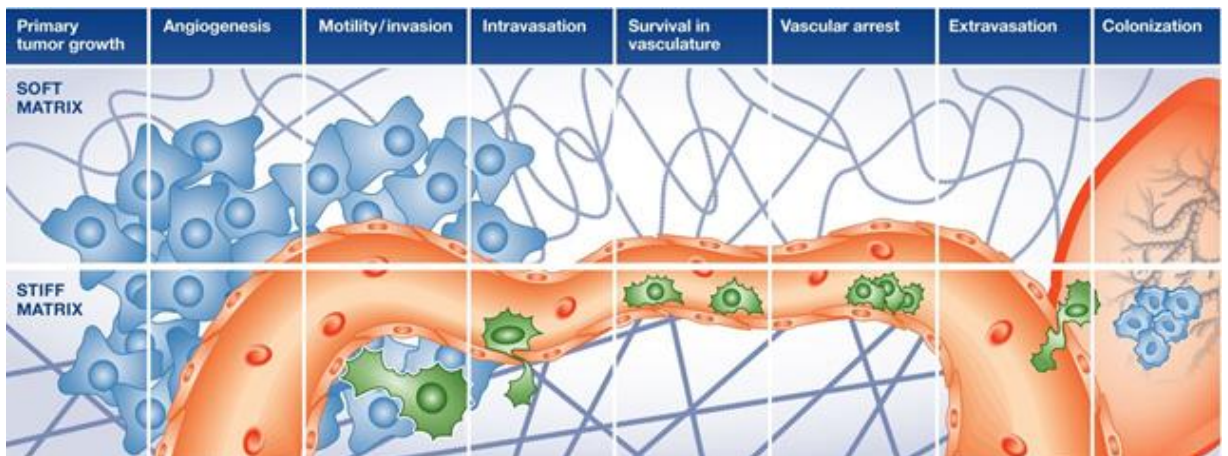


Figure 1.3. Extracellular Matrix and metastasis process relation (Source: Pickup et al.<sup>42</sup>)

## 1.5. Stiffness

The whole integration and barrier features of endothelial cell monolayer are controlled by three major categories. These are contacts of both cell-cell and cell-substrate, soluble intermediary and biomechanics <sup>43</sup>. Examining these inputs and relationship between them has a crucial point for comprehending vascular biology. There are many components that has affected of endothelial cell environment. One of them is substrate stiffness of endothelial cell monolayer. The substrate stiffness shows difference according to various physiologic settings It is increasing with age <sup>44-46</sup>. Also, it is

intensified by some risk factors which were related to common diseases, for example cancer, diabetes, renal disease, hypertension and atherosclerosis <sup>47</sup>. All living structure have a property which is called mechanotransduction and this property is related to physical forces. From simple to complex level of organism has ability to sense and give an answer to these forces <sup>48</sup>. It is known that the cell can behave according to the matrix stiffness in which they are in direct contact <sup>49</sup>. According to recent studies, matrix stiffness has an important role on effecting the cell conducts, such as “cell spreading and adhesion”, “migration”, and “differentiation” <sup>36</sup>. Studies about mechanobiology over the last ten years has proceeded and these studies has combined both biologic and engineering field for better understanding of increasing relation between stiffness of ECM and disease. Although the effect of changes in tissue mechanics in pathological conditions is not yet clearly understood, recently it has observed that changing in tissue stiffness can be apparent before the progression of disease <sup>42, 50</sup>. ECM shows managing the cell fate properties which are viscous and elastics, respectively <sup>51</sup>. ECM stiffness is defined Young`s elastic modulus. It is related to pathological conditions. At the same time, it is a significant factor which is affecting cellular behavior <sup>52, 53</sup>. Recently, researches have investigated to what is the effect ECM on the invasiveness of cancer and they tried to understand whether the ECM could be potential biomarker. Matrix stiffness is one of them <sup>54</sup>.

Some studies show that evidence is scaling up ECM could change both mechanics and functions of cancer and their support tissues of cells <sup>55-57</sup>. Cancer tissues are stiffer than normal tissues, in contrast cancer cells are softer than normal tissues <sup>58</sup>. Tissue stiffness which seen in breast cancer is a significant variable for diagnosis. Cancer cells can show different phenotypes depending on stiffness of their environment and alter both their morphology and behavior <sup>57</sup>. Pazsek et al. examined between stiffness ratio of between normal mammary glands and tumors in different collagen gels for investigating role of matrix stiffness in the behavior of breast tissue <sup>57</sup>. Many breast cancers begin to form in the cell vesicle which are the fundamental anatomical units of mammary glands. In another study was found that long-term mechanical interactions with collagen gel caused organization failure and malignant phenotype in breast cell vesicles. Breaking down of the organization of cell vesicles which interacted the collagen gel is more common and faster than non-interacting ones <sup>59</sup>.

Stiffness of various tissues, materials and surfaces can vary between 102 – 1011 Pa. Stiffness of tissue and organ can vary between 102 and 106 Pa (Figure 1.5.), while

stiffness of materials (Figure 1.4.) which is used in microenvironment can vary (collagen and Matrigel 10<sup>2</sup>-10<sup>3</sup> Pa, alginate and agarose gel 10<sup>3</sup>-10<sup>6</sup> Pa, PDMS (polydimethylsiloxane) 10<sup>4</sup>-10<sup>6</sup> Pa, polyacrylamide gel 10-10<sup>6</sup> Pa, polystyrene > 10<sup>9</sup> Pa). The mechanical properties of materials for used to mimicking the microenvironment is important in terms of representing the stiffness of tissues which can be find in living structure <sup>60, 61</sup>.

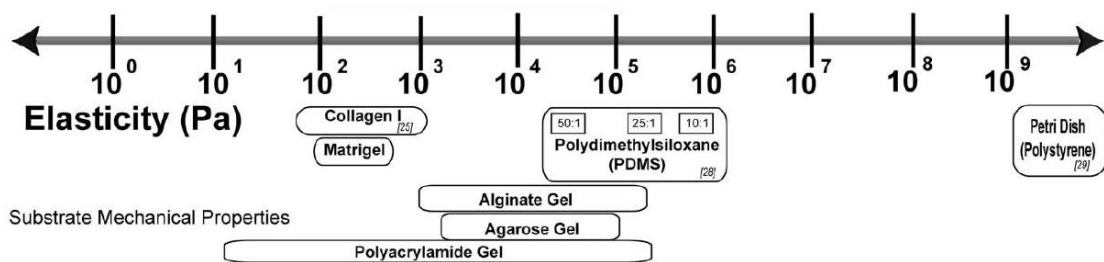


Figure 1.4. Stiffness value of some materials (Source: Kolahi et al.<sup>60</sup>).

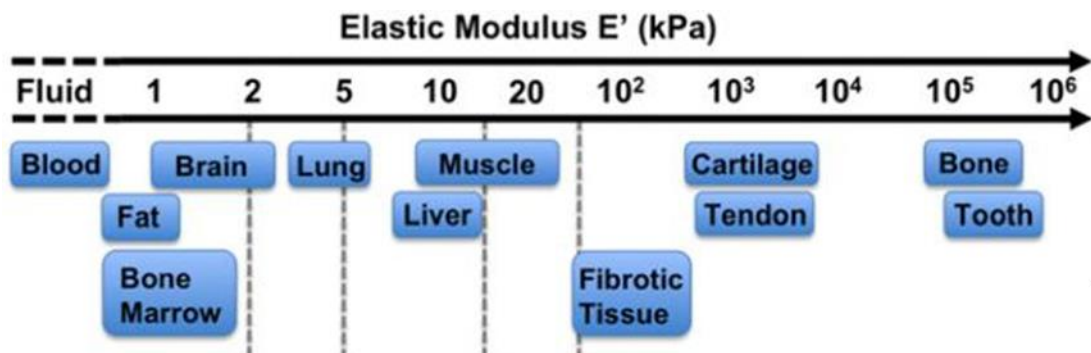


Figure 1.5. Stiffness value of some body organs and tissues (Source: Skardal et al.<sup>62</sup>).

In addition, collagen has a widely usage area as a 3D culture material to investigate a wide variety cell behavior and especially in breast cancer studies <sup>63-66</sup>.

Some defaults of the mechanical properties of tissues may be caused of some cancers <sup>57</sup>. One of these mechanical properties is viscoelasticity which is the most significant one. As a result of this property failure of the tissues, some dysfunctions and complications can be seen <sup>67</sup>. When all these conditions are considered, it is possible to say that viscoelasticity has an important function in the cancer metastasis. In literature, there are some studies have been done *in vitro* before which imitate the fundamental

grades of the *in vivo* process. In addition, most studies have been made usage of two dimensional (2D) models. This method has some usage limitations because of it may not reflect three-dimensional (3D) structure of cell and ECM interactions <sup>68</sup>.

Type I collagen, Matrigel or fibrin which are one of gel type dependent on natural ECM's are consist of proteins. These proteins are sensibly imitating numerous *in vivo* settings because of their self-assemble structure into nanofibrous features *in vitro*. For this reason, these gels are well-defined usage for stiffness studies which mimics ECM <sup>33</sup>. Also type I collagen is significant stress-bearing constituent of both connective tissues and ECM <sup>69</sup>. In addition, collagen is one of the most abundant protein which is find between connective tissues (Figure 1.6.). As a result of some studies in literature <sup>70-72</sup> (Figure 1.7.), collagen stiffness value was changed by using different parameter; such as concentration, pH, temperature, ionic strength and changing of them.

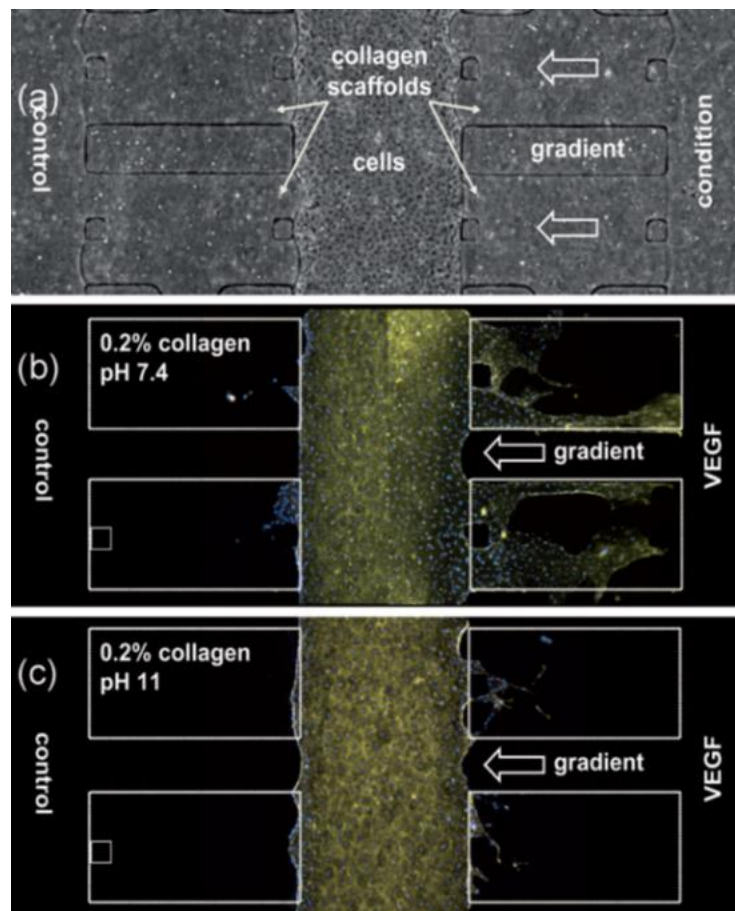


Figure 1.6. Adjusted different pH value of collagen and their effects on migration  
(Source: Chung et al. <sup>71</sup>).

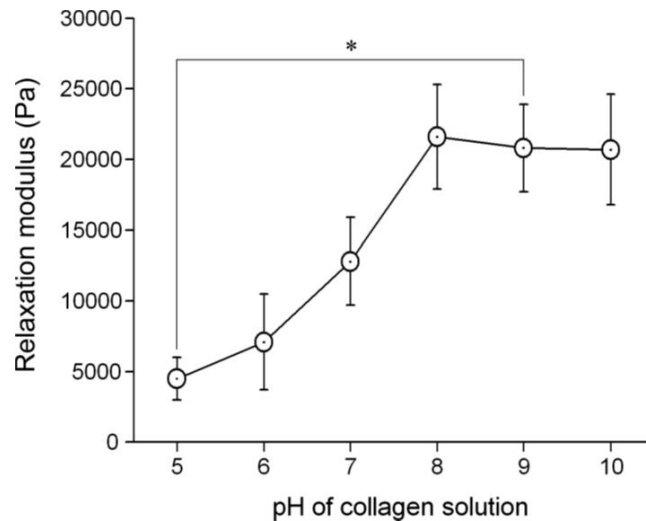


Figure 1.7. Relation between pH of collagen solution and collagen stiffness in relaxation modulus (Source: Yamamura et al.<sup>72</sup>).

## 1.6. Lab-on-a-chip

*In vitro* models have an important role in mimicking the physiological conditions. When the specific interactions such as cancer detailed mechanism want to analyze, these models may be inadequate. In addition, they are not suitable for performing the repeatable studies. Because of these reasons, various *in vitro* models have been evolved to try solving these problems<sup>73</sup>. *In vitro* models cannot fully mimic the *in vivo* situation due to some limitations. However, they can tolerate these limitations because of some features. They do this by providing controllable environments in which single culture parameters can be altered and using human cells<sup>74</sup>. Some traditional assays such as Boyden chamber and wound healing assay have been used in a large area for biological researches such as cancer and drug screening. However, there are some reasons that limit their usage. They cannot provide adequate control over the microenvironment that is being created, and the analyzes to be performed cannot be efficiently occurred due to complexity and imaging can be limited<sup>75</sup>. The microfluidic field has recently started to be used in the biology area to minimize these limitations. They have been enhanced to use of controlling the both cell and tissue microenvironment. This situation has made it possible for biologically based research to become widespread<sup>76</sup>. Bioanalytical systems which are based on both micro and nanotechnology are called micro devices. They have been revolutionized the

biological research field. Also, they have many advantages that consist small structure sizes and high sample processing capacity <sup>77</sup>. These systems defined as lab-on-a-chip systems (Figure 1.8.). LOC systems reduce the costs, increase reproducibility and accelerate the examine the strength and stability of pharmaceutical compounds, investigation of disease mechanisms and evaluate toxic compounds in models that is more human intimated. They can mimic the tissue or organ systems of human. Because of this future, it could minimize of requirement for animal testing in preclinical research area <sup>78</sup>. LOC devices try to solve some technical issues which were created by other traditional assays. They give an opportunity to create controllable both biochemical and biophysical 3D microenvironment and this combined with real time screening. Because of this, LOC systems have a broad range in cancer researches, especially in cancer metastases <sup>79</sup>. For this purpose, various LOC devices have been improved to research cancer cell metastases steps. Such as “invasion and migration”, transition effects of the cell according to “mechanical barriers”, “intravasation”, “adhesion” and “extravasation steps” <sup>75</sup>.

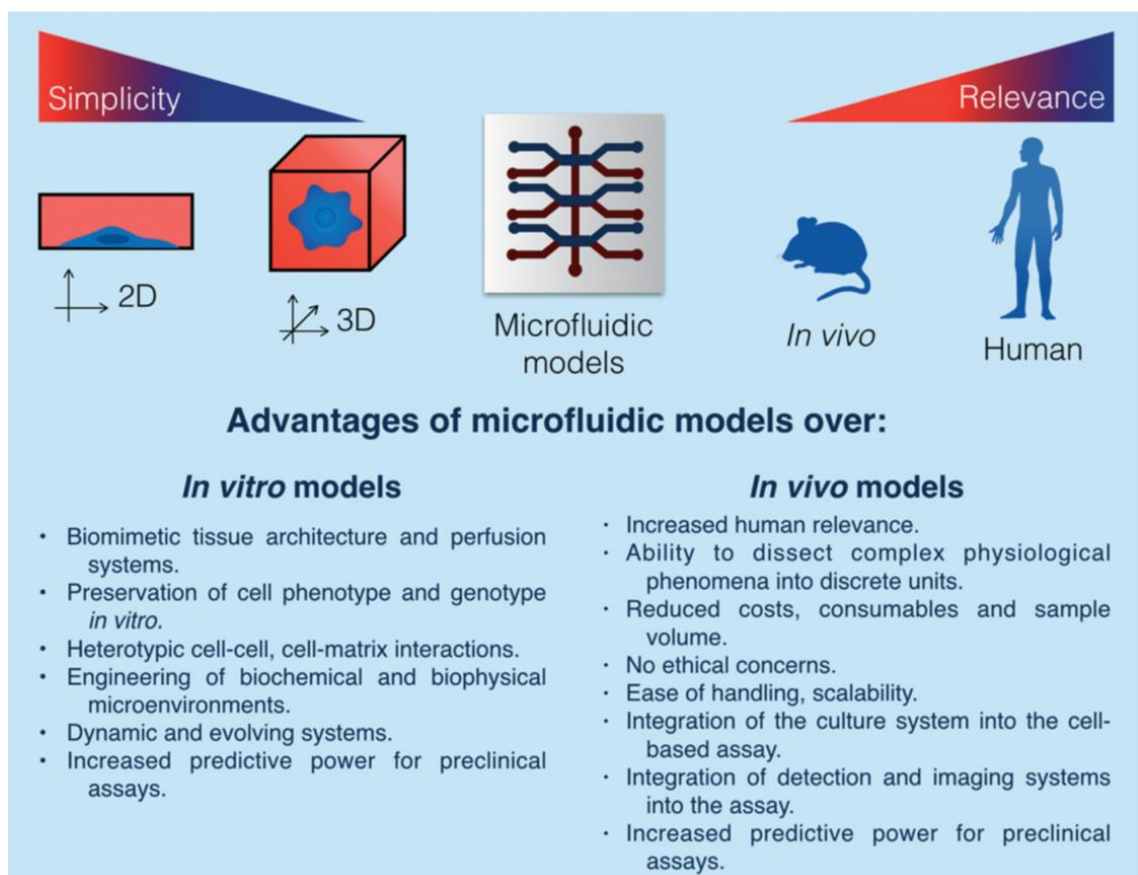


Figure 1.8. Comparison of in vitro and in vivo models (Source: Partillo-Lara et al.<sup>80</sup>).

## **1.7. Aim of the Study**

It is unclear whether mechanical properties of collagen matrix underneath endothelial cells affect MDA-MB-231 – MCF10A cell lines extravasation under the static and perfusion flow condition. In this study changing pH value of collagen was mimicked the different matrix stiffness condition. To applied static and perfusion flow condition were applied to provide different conditions. The aim of the project was to determine extravasation efficiency as a function the mechanical properties of matrix underneath endothelial cells in lab-on-a-chip devices.

## CHAPTER 2

### MATERIALS AND METHODS

#### 2.1. Cell Culture

Cell culture is a kind of biological process. Cells are isolated from living tissues. Then these cells are kept control under the specific conditions and are made prepare to be use in proper experiments.

##### 2.1.1. Medium Preparation of bEnd.3 Cell Line

bEnd.3 (mouse brain endothelial cell line) was obtained from ATCC. Dulbecco's Modified Eagle Medium (DMEM) (Biological Industries, Cat No 01-055-1A) was used to provide medium for bEnd.3 cells. Before the preparation steps; DMEM was placed from +4°C to room temperature and other ingredients were placed from -20°C to water bath. In the preparing process, 450 ml of DMEM and 50 ml (10%) Fetal Bovine Serum (FBS) (Biological Industries, Cat No 04-001-1A) were mixed in 1:10 ratio. Then, 5 ml (1%) Penicillin – Streptomycin (Biological Industries, Cat No 03-031-1B) and 5 ml (1%) L-glutamine (Biological Industries, Cat No 03-020-1B) were added. Bottle was shaking gently up and downside and filtered in PES filter system (Corning, Cat No 431097). Storage temperature of medium was +4°C.

##### 2.1.2. Medium Preparation of MDA-MB-231 Cell Line

MDA-MB-231 (breast cancer cell line) was obtained from ATCC. Dulbecco's Modified Eagle Medium (DMEM) (Biological Industries, Cat No 01-055-1A) was used to provide medium for MDA-MB-231 cells. Before the preparation steps; DMEM was placed from +4°C to room temperature and other ingredients were placed from -20°C to water bath. In the preparing process, 450 ml of DMEM and 50 ml (10%) Fetal Bovine



Serum (FBS) (Biological Industries, Cat No 04-001-1A) were mixed in 1:10 ratio. Then, 5 ml (1%) Penicillin – Streptomycin (Biological Industries, Cat No 03-031-1B) and 5 ml (1%) L-glutamine (Biological Industries, Cat No 03-020-1B) were added. Bottle was shaking gently up and downside and filtered in PES filter system (Corning, Cat No 431097). Storage temperature of medium was +4°C.

### **2.1.3. Medium Preparation of MCF-10A Cell Line**

MCF10A (breast epithelial cell line) was obtained from ATCC. Dulbecco's Modified Eagle Medium (DMEM F12/HAM 1:1) (Biological Industries, Cat No 01-170-1A) was used to provide medium for MCF10A cells. In the preparing process, 13 ml DMEM F12 was added 25 ml 5% Donor Horse Serum (DHS) (Biological Industries, Cat No 04-004-1A) and mixed. Then, 100 microliter 2ng/ml Epidermal Growth Factor (EGF) (Sigma, Cat No E9644), 250 microliter 0.5 um/ml Hydrocortisone (Sigma, Cat No H0888), 500 microliter 10 ug/ml insulin (Sigma, Cat No I1882), 50 microliter 100 ng/ml Cholera Toxin (Sigma, Cat No C8052 – 0.5MG), 5 ml (1%) Penicillin – Streptomycin (Biological Industries, Cat No 03-031-1B) and 5 ml (1%) L-glutamine (Biological Industries, Cat No 03-020-1B) were added respectively. In final step the mixture was added DMEM F12 bottle. It was shaking gently up and downside and filtered in PES filter system (Corning, Cat No 431097).

### **2.1.4. Cell Passage**

At the beginning of the cell culture, the cell specific medium (10ml) was added to 100x20mm petri dishes (treated) and were placed to incubator at 37°C, %5 CO<sub>2</sub>. The confluency of the cells to be passaged were checked under the microscope and the cells that reached the enough density were taken to the laminar flow cabinet for passage. Medium was pulled by vacuum and added 2 ml Trypsin-EDTA (type A or C) solution each petri dish then it was aspirated immediately to separate attached dead cells. In here, trypsin-A (Biological Industries, Cat No 03-050-1B) for bEnd.3 cells and trypsin-C (Biological Industries, Cat No 03-053-1B) for MDA-MB-231 and MCF10A cells was used. Then, trypsin solutions were added again to provide detaching cells and petri dishes

were placed into incubator. Incubation period was for 3 minutes, 5 minutes and 17 minutes for bEnd.3, MDA-MB-231 and MCF10 cells, respectively. At the end of the incubation period, cells were controlled under the microscope to check whether the cells up or not. Then petri dishes were placed into cabinet and added 1 ml cell specific medium for blocking the effect of trypsin solution. This solution was washed gently by pipette and 5 ml solution was added to 15 ml falcon tube. Petri dishes were controlled under the microscope again. Then 5 ml medium was added and tried again washing step and added falcon tube. Centrifuge step was applied for 5 minutes at 1000 rpm to precipitated cells at the bottom of the falcon tube. After centrifugation, cells supernatant was pulled with vacuum and 1 ml medium was added to dissolve the cells pellet. Pellet-medium mix was split accordingly determined ratio for each cell type and added to new treated petri dishes. Subcultivation ratio of cells were; 1/6 - 1/10, 1/2 - 1/4, 1/4 - 1/8 for respectively bEnd.3, MDA-MB-231 and MCF10A cell lines. After these steps, petri dishes were shake gently in X – Y direction for separation of equal ratio of cells in medium. Lastly, petri dishes were put into incubator at 37°C, %5 CO<sub>2</sub>.

### **2.1.5. Cell Thawing**

Firstly, 60 mm petri dish was filled with the cell's medium to be used and put into 37°C and 5% CO<sub>2</sub> incubator before starting to be thawing process. Water bath was adjusted 37°C. After the temperature reached, Cryogenic vials (Corning, Cat No CLS430487) was gotten from the liquid nitrogen tank or -80 °C and they were placed into water bath until the cell mix solution were thawed complete. Then this 1 ml cell solution were added to falcon that consisted 9 ml medium and falcon was centrifugated for the purpose of separated Dimethyl Sulfoxide (DMSO) (Sigma, Cat No D2650-5X5ML) from the cells. 1 ml culture medium was used to dissolve the cells and then cells added to petri dish. After the two passage were passed, cells were ready to use experiments. Cells were controlled under the microscope every day and changed their medium according to their confluency. After the two passage were passed, cells were controlled under the microscope. If cells were shown enough confluency, they were became ready to use in the experiments.

### **2.1.6. Cell Freezing**

At the end of the passage process, cells were dissolved 1 ml culture media. In other falcon, DMSO solution prepared to be 7.5% of total working volume (2ml). Prepared mixture was added drop by drop to keep away from shocking to cell. The total volume was transferred into two cryo tubes with a half volume. Cryogenic vials (Corning, Cat No CLS430487) were placed to -20 °C for a few hours and -80 °C for overnights, respectively.

### **2.1.7. Cell Tracking**

The amount of Cell Tracker™ Green CMFDA (5-chloromethylfluorescein diacetate) (Invitrogen, Cat No C2925) and Cell Tracker™ Red CMTPX (Invitrogen, Cat No C34552) in stock was completed in volume with DMSO according to their known molecular weight and how much concentration it would use. In experiments, green and red trackers were diluted 1:1000 ratio with cell type specific media to be reduce the concentration to 5 µM and 10 µM. Briefly, the media from petri dish was withdrawn by vacuum and washed with 2 ml serum-free medium 3 times and took with vacuum per washing. The dye – medium mixture was added to petri dish and petri was placed to 37°C and 5% CO<sub>2</sub> incubator for 45 minutes. Stained cells were taken from incubator and washed 3 times with serum – free medium again. Lastly, cell specific medium was added to petri dish and checked under the fluorescence microscope (ZEISS) to observe for staining.

## **2.2. LOC Device Fabrication**

Lab-on-a-chip devices were widely used in biological research area. There are many different techniques to fabricate LOC devices. In addition, different steps were applied during this fabrication process.

### 2.2.1. UV – Lithography

UV lithography method was used to create molds for the design of the LOC devices. In order to create three-dimensional LOC devices were used in all experiments, polydimethylsiloxane (PDMS) polymer was exposed to UV light and various sub-steps were performed to prepare molds for three days and these methods were based on previous studies <sup>81</sup>. All process was performed in Applied Quantum Research Center Clean Room (Department of Physics, Izmir Institute of Technology). SU-8 2075 negative photoresist (Microchem, USA) master mold was formed. In this method, silicone surface was preferred because this surface was more capable for SU-8 based polymers when comparing the glass substrates. Silicon wafers were used as a substrate with a 100 mm diameter (University WAFER, Cat No 452). On the first day, heater (WiseStir® MSH-20D, DAIHAN Scientific, Korea) was adjusted 65 C° and then silicon wafers were left on heater for 5 minutes. Thus, SU-8 was homogenously spread over the heated surface. A few amounts SU-8 was poured onto heated silicon wafer and right after that silicon wafer was gently shook in elliptic orbit for homogenous distribution of SU-8. Then silicon wafer was placed onto spin coater machine (G3P-8 Desk-Top Precision Spin Coating System, Specialty Coating Systems, Indianapolis, IN) to complete the dissemination process. 1000 rpm with 50 ramp and 25 dwell mode were applied to obtain the thinner height of wafer. Silicon wafer was placed onto 65 C° for 5 minutes and 90 C° for 1 hour respectively. After heating process, wafer was taken on the counter and was left to cool for the second day. Next day of UV lithography, wrinkle test was applied wafer to check the suitability of the baking steps. In this test, heater was adjusted 95°C and wafer was placed on heater. If the baking steps were applied incorrectly, wrinkles were observed on wafer. Wafer was placed on bench for minutes and replaced on heater again. Heating process was repeated until the wrinkle was not seen. At the same time, two heaters were adjusted 65 °C and 90 °C respectively. Wafer was waited at room temperature (24 °C for 5 minutes). In the meantime, UV mask aligner (OAI Hybralign Series 200, San Jose, CA) which was provided to press a mask mold via using UV light, was controlled and aligned using a water balance. Vacuum option of mask aligner was activated, so wafer was anchored. Specific mask design was made in Corel Draw program and printed on acetate paper. Bright side of mask mold which was pressed on the SU-8 photoresist was placed on wafer and strapped with transparent tape. Thus, only

determined area was exposed with UV light. UV light was applied only 30 second. When the exposure time was increased, overexposure was observed or subsequent steps of third day were not completed. Polymerization process was occurred only areas which were exposed UV light because of SU-8 is negative photoresist. At the end of the exposure step, wafer was placed heater at 65 °C for 5 minutes and 90 °C for 10 minutes respectively. Lastly, wafer was put on counter and kept at room temperature until for subsequent steps of next day. On the last day steps purpose was to clean unexposed UV light area of SU-8 photoresist with developer and this step called developer step. For this, wafer was placed in glass petri dish which was filled SU-8 developer solution (Microchem, USA) and kept in this solution for 5 minutes without shaking. At the end of 5 minutes, petri dish was shaking gentle circular orbit for 20 minutes. After this step, the edge of wafer was checked by isopropanol dripping (IPA Test) (Merck, Cat No 109604) in order to observe whether the unexposed UV light areas were cleaned or not. When the white color was seen, it meant that target areas were not cleaned completely. Developer solution was refreshed, and wafer was put in again for 5 minutes. At the end of time, wafer was tested again with isopropanol and checked under the microscope (Nikon, Japan) which were supported specific photonic optics (PL 2000) to observe whether the desired shape was formed or not. Lastly, wafer was washed with isopropanol for block the developer effect and dried with dust free napkin, so SU-8 wafer was become ready to use.

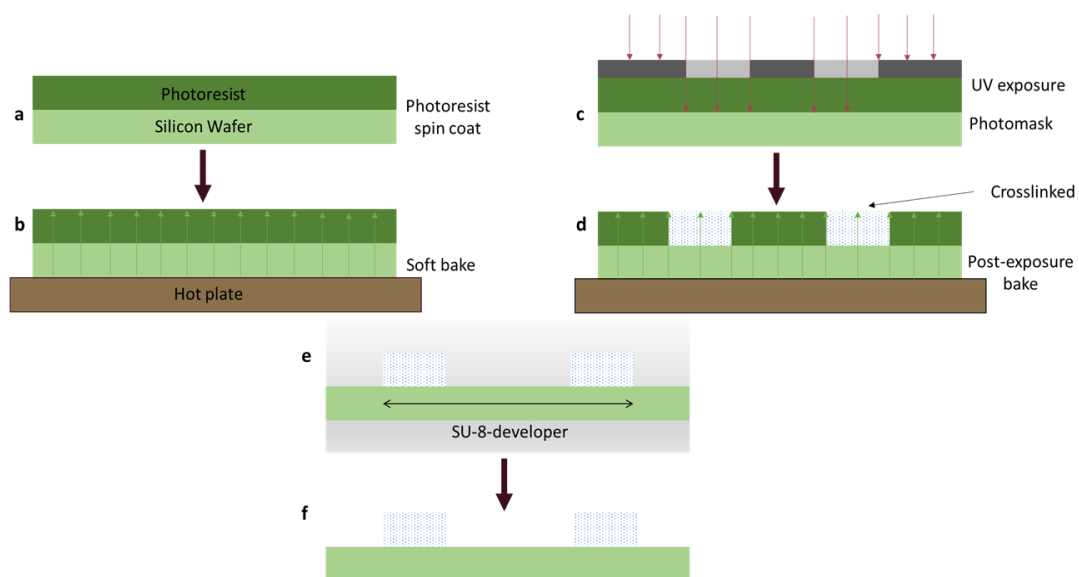


Figure 2.1. The fabrication process of UV Lithography.

### **2.2.2. Polydimethylsiloxane (PDMS) Molding**

Before the molding process, SU-8 master mold was cleaned deionized water ( $\text{dH}_2\text{O}$ ), ethanol (EtOH), demolding agent and left to bench for drying. Then wafer cover was prepared by using aluminum foil. SU-8 wafer was anchored aluminum cover via double sticky type. PDMS molds were formed by using polydimethylsiloxane (PDMS) elastomer. In this process, 184 silicone base elastomer and curing agent kit which were settled by SYLGARD® (Dow Corning, Midland, MI, U.S.A) was used and mixed in a 1:10 ratio by weight. For this, a plastic cup was placed on analytical balance and took tear. Total amount of PDMS was 60 gram per wafer and this amount was consisted 54-gram silicone elastomer and 6-gram curing agent respectively. Then the mixture was mixed until the bubbles were observed. Desiccator (PlusMED, 7E-A, Danyang, P.R.C) was used to eliminate bubbles in the mixture. At the end of vacuum step, PDMS mixture was poured on SU-8 wafer and left to complete polymerization for 2 days. After polymerization step was completed, SU-8 wafer and PDMS were uncoupled from each other.

### **2.2.3. PDMS Punching and Cleaning**

During punching step; the PDMS cut separately from each design. The cut PDMS's were punctured at appropriate sizes according to their intended use in future experiments. These holes provided to load for chips. While the inlet and outlet holes were drilled, and the chips were made ready for cleaning. PDMS molds cleaning step is the most significant part of sterilization process. Firstly, scotch tape was used to remove dust particles from PDMS molds. The cut and punched PDMS molds were placed into glass slide holder with the pattern portions were placed facing up. During the cleaning steps; PDMS molds were cleaned one time with ultra-pure water ( $\text{UpH}_2\text{O}$ ), ethanol (EtOH) and again ultra-pure water, respectively. Then, ultra-pure water ( $\text{UpH}_2\text{O}$ ) was added to cover all the PDMS molds and left for 10 minutes in sonicator (WiseClean, WUC-A03H, DAIHAN Scientific, Korea). At the end of the sonication, it was washed 5 times with ultra-pure water. For re-sonication, 70% ethanol was added to glass slide holder and sonicated for 5 minutes. Afterwards, it was washed twice with 70% ethanol and filled

with ethanol again and put on bench for 5 minutes. Finally, it was washed one last time with ultra-pure water. After the washing process, the water drops on the PDMS molds were taken with the help of desiccator. Cleaned filter paper was placed into glass petri dish and PDMS molds were put in there. Then it was lifted to oven (NÜVE STERILIZER, FN 032, TURKEY) at 37° C to dry.

#### **2.2.4. PDMS Bonding**

Glass microscope slides were cleaned following the protocol before bonding process. Slides were lined up in glass slide holder and then methanol for one day, ultra-pure water (UpH<sub>2</sub>O) for second and third day were added respectively. Lastly, slides were lifted to 60° C to dry.

The PDMS molds, which were subjected to punching and cleaning process, were re-cleaned with scotch tape before bonding process. The patterned side of PDMS mold and clean glass microscope slide which is pasted were placed into UV/Ozone cleaner (BIOFORCE NANOSCIENCES, UV/Ozone ProCleaner™ 220). Then they were exposed under UV for 5 minutes. PDMS mold which was interacted to ozone treated changed their structure from hydrophobic to hydrophilic for permanently bonding. The ozone-exposed patterned side of the PDMS from the device was adhered to the glass. After these step, PDMS mold and glass bonding were controlled to whether bond or un-bond. If there are non-bonding parts, they were pressed by tweezers so as not to damage the pattern. Then LOCs were placed to heater at the 100°C for 15 minutes. Lastly, they were exposed with UV light for sterilization in laminar cabinet for 15 minutes. At the end of this step, LOCs were put on glass petri dish at room temperature.

#### **2.2.5. Channel Height Measurement**

Vertically section was obtained from polymerized PDMS mold and taken a photo under the phase - contrast microscope at 4X objective. Black strips were used as a scale for measurement and their photo were also taken under the same microscope. ImageJ / Fiji software were used to measure for channel height. Following steps were applied to find channel height respectively. Two points are drawn by selecting the straight line to

find the pixel value of distance between the two strips. Pixel value were found via analyze-measure/measure section. Same process was also applied to PDMS vertical section. In last step, the distance between the measured pixel value and the measured pixel value of 200 micrometer was calculated by proportional ratio.

### **2.3. LOC Device Coating**

Before coating step, all chips that were completed whole preparation steps were treated with UV for 15 minutes to sterilization. APTES was prepared with using acetone at 2% ratio and loaded into the flow channel and kept laminar flow cabinet at room temperature for 15 minutes. Then it was pulled with vacuum and washed three times with 1x PBS and upH<sub>2</sub>O, respectively. Poly-L-lysine (PLL) was prepared with using ddH<sub>2</sub>O and final concentration was 0.1 mg/ml. PLL loaded into the flow channel and placed into incubator 37°C %5 CO<sub>2</sub>. Then it was pulled with vacuum and washed three times upH<sub>2</sub>O. After APTES or PLL coating, it was coated with different proteins which were Laminin (0.0125 mg/ml), Fibronectin (0.0125 mg/ml) and type I Collagen (50µg/ml). They were placed to incubator 37°C %5 CO<sub>2</sub>. At the end of the incubation, all proteins were pulled with vacuum and washed three times with UB and upH<sub>2</sub>O, respectively. Different coated LOC devices were placed into a vacuum desiccator overnight for preservation of the protein coating until used in the experiments.

### **2.4. Dextran Preparation**

Dextran is a kind of a polysaccharide and it has a high molecular weight glucose polymer. It shows high water solubility and low toxicity properties. Dextran 450-600 kDa from *Leuconostoc* spp. (Sigma, Cat No 31417-100MG-F) was prepared in 8% ratio with bEnd.3 medium and put on shaker for dissolve homogenously in medium. After the dissolving process was completed successfully, it was filtered to become a sterile. Dextran transferred to pellet in the falcon tube for dissolved during the experimental process.



## **2.5. Gel Preparation**

In these steps' different structures such as Matrigel and collagen were used to mimic extracellular matrix. Matrigel is a commercial name of protein mixture which is produced by mouse sarcoma cells. Collagen is a kind of protein which is found in connective tissue.

### **2.5.1. Matrigel and Collagen Preparation**

Growth factor reduced Matrigel (Corning, Cat No 356234) was diluted with DMEM High glucose medium in 1:1 ratio and final concentration was 4 mg/ml. Matrigel was loaded matrix channel of LOC devices and was placed into 37°C, 5% CO<sub>2</sub> incubator for gelation process for 35 minutes. Type I Collagen (Corning, Cat No 354236) was obtained from RTT and solubilized at 9.66 mg/mL in 0.02M acetic acid. Collagen was consisted 10X PBS, 0.1 M sodium hydroxide (NaOH) and ultra-pure H<sub>2</sub>O. Amount of 10X PBS was 10% of added total gel mixture volume. Gel was prepared corresponding different pH's according to adding different amount of NaOH. Final volume was adjusted with using upH<sub>2</sub>O and all collagen concentration was constant in whole different pH values which was 3 mg/mL. Collagen was loaded matrix channel of LOC devices and was placed into 37°C, 5% CO<sub>2</sub> incubator for gelation process. This process was completed 1 hour.

### **2.5.2. Collagen pH Measurement**

Collagen gels were prepared according to protocol which is mentioned above and were placed into eppendorf tubes. All eppendorf tubes were kept on the ice cube to avoid polymerization. pH papers were used to measure of collagen gel pH's. For this reason, 20 microliter amounts were taken each collagen condition and put onto pH papers drop by drop. After a few seconds color changes were observed and determined the exact pH's of all collagen gels condition. Two different conditions which were represented low pH (soft

one) and high pH (stiff one). So, different stiffness value of extracellular matrix was mimicked according to change pH value of type I Collagen.

## **2.6. Endothelial Monolayer Formation**

bEnd.3 cell line was passaged and stained by green tracker. Cells were suspended with using Dextran or own medium. After that, cells were counted with using EVA Automatic cell counter (NanoEntek) according to determined calculation and prepared the suspension of cell numbers for each LOC devices suspension was loaded softly into flow channel. They were placed into glass slide holder vertically and put into 37°C and 5% CO<sub>2</sub> incubator overnight. After overnight incubation, all LOC devices were displayed with using confocal microscopy. In here, 488 fluorescence light was used to observe bEnd.3 cells whether they were formed monolayer successfully. All posts of LOC devices in different position were taken.

## **2.7. Endothelial Monolayer Integrity**

Dextran, Tetramethylrhodamine, 70 kDa (Life Science, Cat No D1819) was used for both under the static and flow conditions to control endothelial permeability whether cells were formed monolayer successfully. At first step, endothelial monolayer was formed and viewed according to introduce previously. Then dextran diluted with DMEM High Glucose in 1:250 ratio. Before loading the dextran, all LOC devices photos were taken by using fluorescence microscope (Zeiss, Germany). In static conditions; LOC devices matrix and reservoir channels were closed with double-sided tape and used mineral oil drops for avoid evaporation. Dextran was loaded flow channel and LOC device was placed into fluorescence microscope (Zeiss, Germany). In flow conditions, same dextran loading process was applied but in here LOC devices were placed on rotator in incubator. In specific time intervals minutes LOC devices photos were taken by using fluorescence microscope.

## 2.8. Perfusion

According to P. Morier et al. study, gravity driven flow rate was formed with according to height changes which were depend different angle <sup>82</sup>. This method was chosen because of keep under the control the monolayer without any damage. Based on this method, LOC device were placed on rotator (Multi BioRad RS-24, BioSan) and different angles were tested that were 5°, 10°, 15° and 20° respectively in 1 rpm. Photos were taken at start and finish place of center to determine the correlation between angle and height (Figure 2.2.). Their appropriate value was calculated in Image J. A graphic showed that changes the between angle and height relation (Figure 2.3.). In addition, shape of microchannel of LOC device was rectangular, also flow rate and pressure difference were calculated with using these Pouseille Flow formula <sup>83</sup>;

$$Q \approx \frac{h^3 w \Delta p}{12 \eta L} \left[ 1 - 0.630 \frac{h}{w} \right], \text{ for } h < w \quad \Delta P = \rho g h$$

In this formula; Q is volumetric flow rate (m<sup>3</sup>/s), h and w are height and width (m),  $\Delta p$  shows pressure differences (Pa),  $\eta$  shows viscosity (Pa\*sec) and L is length of the channel (m).

In addition to this formula, shear stress of wall must be known because of preserving the monolayer structure. Shear stress which acts external force to surface were calculated according to this formula <sup>84</sup>;

$$\tau = \frac{6 \eta Q}{w h^2}$$

In this formula; “ $\tau$  is the shear stress (dyn/cm<sup>2</sup>),  $\eta$  the dynamical viscosity (dyn/cm<sup>2</sup>), Q is the flow rate (cm<sup>3</sup>/s), h is the height of channel (cm), and w is the width of the channel (cm)”. When combined all, total changes in height which was referred delta H was reverse ratio in height of microchannel. Calculation of shear stress gave to appropriate angle which were used in rotator. Degree were determined by using these formulas and flow were applied 4 hours.

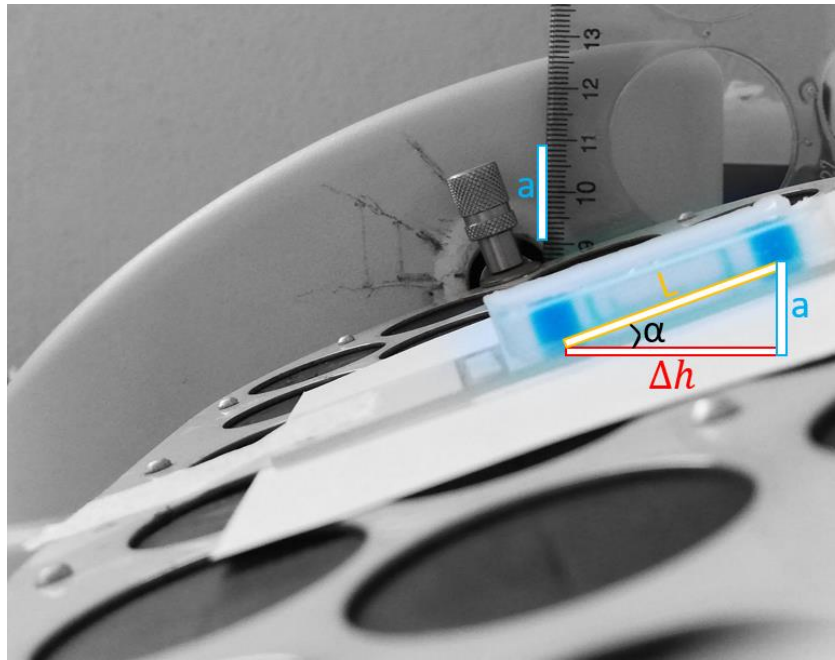


Figure 2.2. Image represent height difference of LOC devices according to angle.

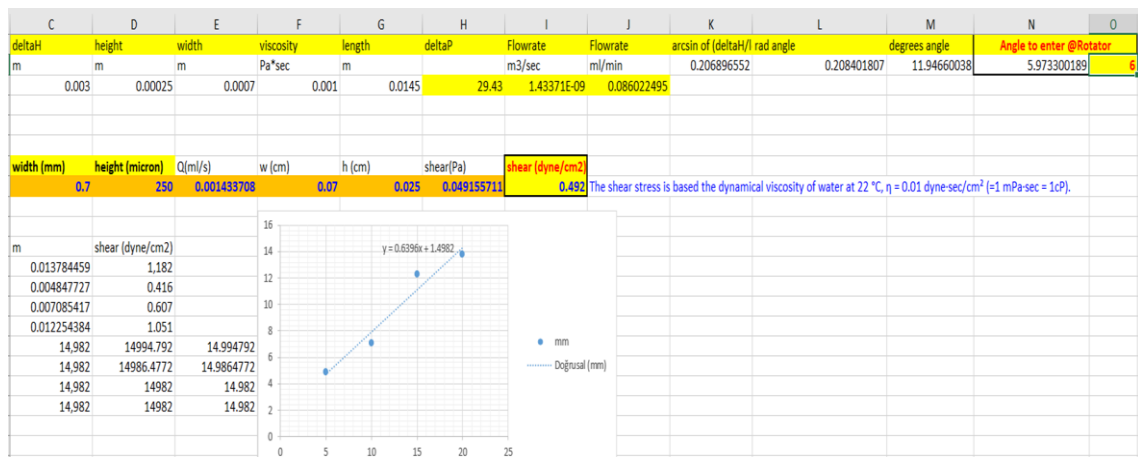


Figure 2.3. Shear stress and angle calculation according to height differences and flow rate values.

## 2.9. Extravasation Quantification

Completion time of extravasation experiment for both static and flow conditions was 24 hours. Then Z-stack photos were taken from each post of the LOC devices in the 10X lens with a gap of 15.04  $\mu\text{m}$  along the channel height. Photos of bEnd.3 which was labeled with green tracker and MDA-MB-231 / MCF 10A which were labeled red tracker were taken in 488 nm and 555 nm wavelength, respectively in confocal microscope. Their

Z-stacks photos were merged and set to maximum intensity mode which was represented in 2-dimensional structure. In that mode; endothelial monolayer which was formed in each post of LOC devices was accepted as a boundary. According to this boundary, extravasation analyses was applied for both MDA-MB-231 and MCF 10A cell lines. These cells were separated 3 different groups which were “extravasated”, “associated” and “flow channel”. If the cells were passed thorough the monolayer it was called extravasated, in contrast of the cells were interact with endothelial monolayer it was called associated. In addition, the presence of cells in the flow channel was referred to as the flow channel. Afterwards, the photos of LOC devices were taken along the channel heights in Z direction were converted 3-Dimensional photos and checked at different angles in Las X which were in simulation mode.

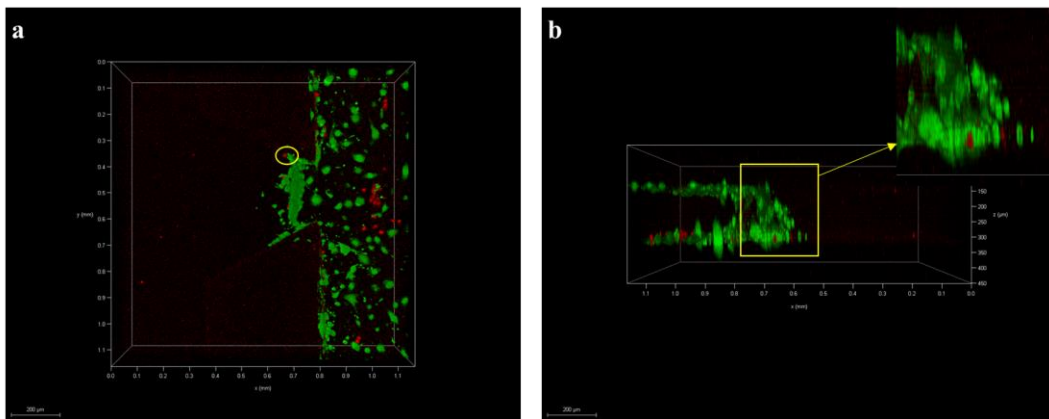


Figure 2.3. a) Yellow circle shows extravasated cell in vertical view of endothelial monolayer. b) Zoom in extravasated cell in horizontal view of endothelial monolayer.

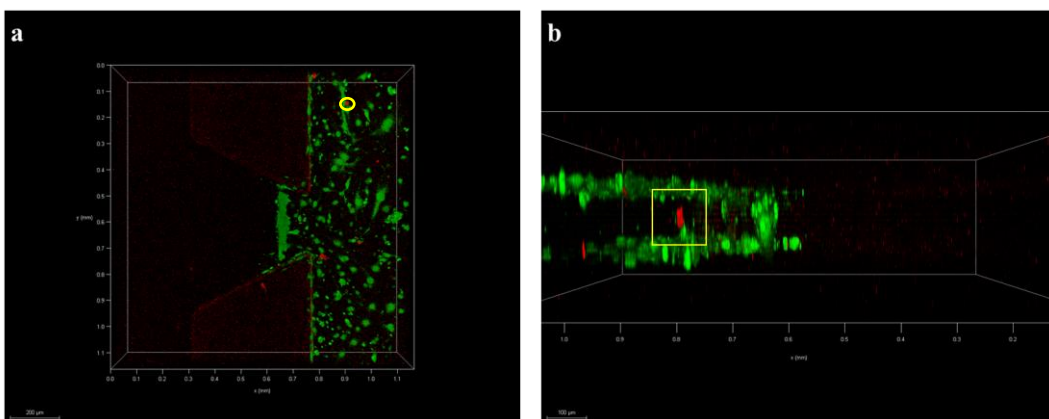


Figure 2.4. Cells in endothelial monolayer represents in flow channel. a) vertical view of endothelial monolayer. b) horizontal view of endothelial monolayer.

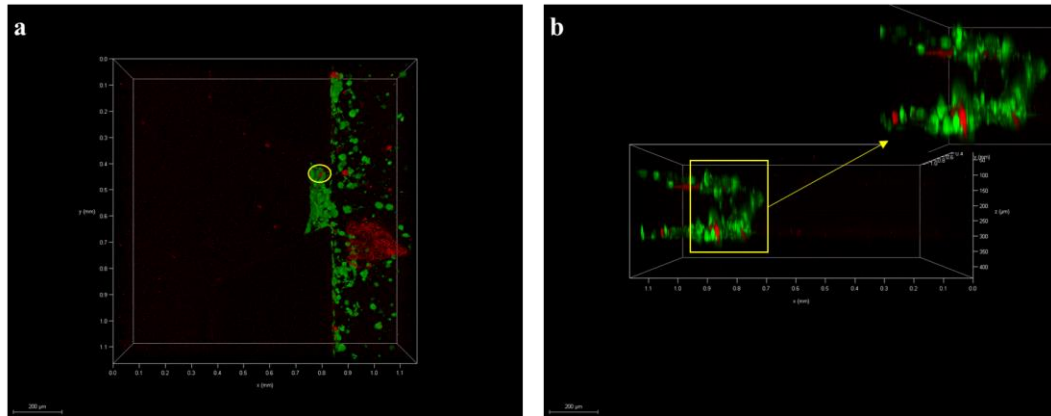


Figure 2.5. a) Yellow circle shows associated cell in vertical view of endothelial monolayer. b) Zoom in associated cell in horizontal view of endothelial monolayer.

## 2.10. Distance of Extravasated Cell Quantification

For extravasated cells, how much of each cell migrated from the starting point of endothelial monolayer according to vertical distance was calculated in  $\mu\text{m}$  with using Leica Las X program. In first step extravasated cells were controlled in 3D mode. Then 2D mode was opened and 3 channels which are brightfield, 488 and 555 fluorescence are merged. Max intensity option was applied, and Z position was changed to show the extravasated cells clearly. To calculate the distance straight line was drawn between the endothelial monolayer and extravasated cell. These steps were applied to all post in experiments (Figure 2.6.).

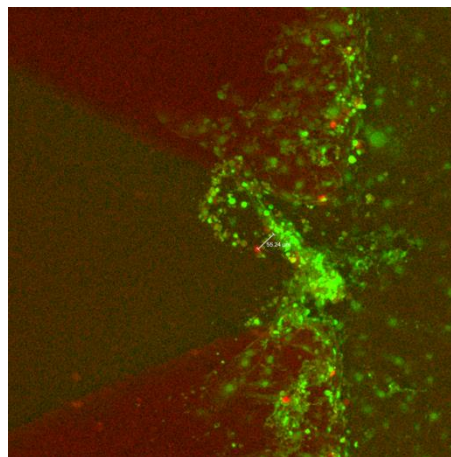


Figure 2.6. Representative image shows that distance of extravasated cell from the endothelial monolayer.

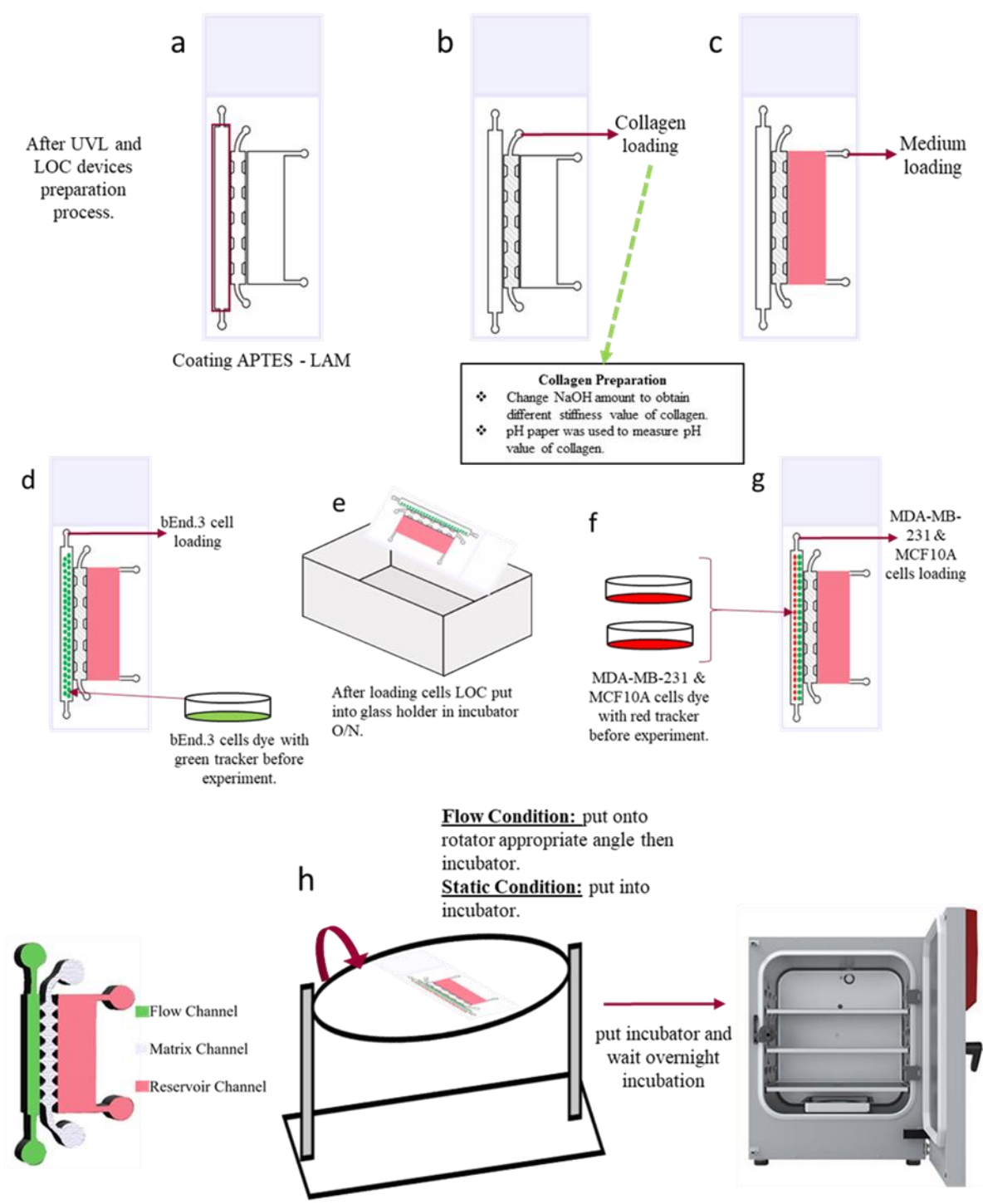


Figure 2.7. Experimental flow scheme.

## CHAPTER 3

### RESULT AND DISCUSSION

#### 3.1. LOC Device Fabrication with using UV Lithography Method

UV Lithography technique was used to manufacture of SU-8 wafers (master molds). PDMS-LOC devices were fabricated by using these master molds. LOC devices were prepared by applying following steps punching, cleaning, bonding and sterilization. Height of LOC devices were varied, and width is 1 mm for flow channel. In this design, there are three channels which were entitled flow, matrix and reservoir respectively. Different sizes of punches were used to form inlets and outlets in LOC devices. Inlets and outlets of flow channel are 2 mm, and both of matrix and reservoirs are 1.5 mm (Figure 3.1.).

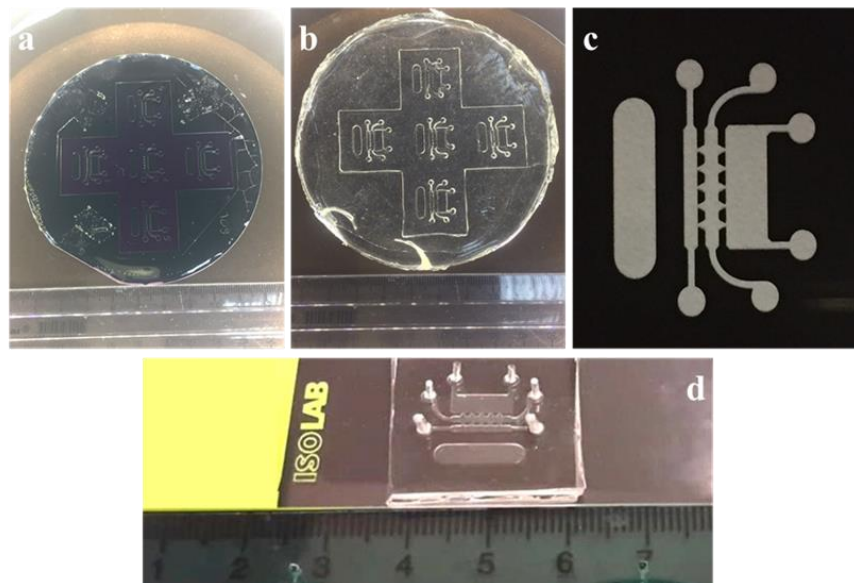


Figure 3.1. a) Image of SU-8 mold (wafer). b) Image of PDMS of Lab-on-a-chip device. c) Design of mask. d) Image of PDMS LOC device after permanent bonding onto glass slide by UV/ozon treatment.



### 3.2.Determination of Collagen pH

During the all experiments, the amounts of the other components were kept constant and only the NaOH component was modified. At first stage, appropriate pH values were tried to find. To change the stiffness of collagen depending on pH value, both different NaOH amount and two different molar concentrations were tried (Figure 3.6.). NaOH was prepared as 0.1 M was divided 3 main different amount experimental groups.

In first group: samples were prepared by varying the amount of NaOH between 1 and 7 microliters in 100 microliter total collagen mixture. Each collagen samples were measured two different types of pH papers which were measure range value between 7.5 – 14 and 0 – 14. Because of the amounts of NaOH were too close, pH results were shown only a few values changing (Figure 3.2.).

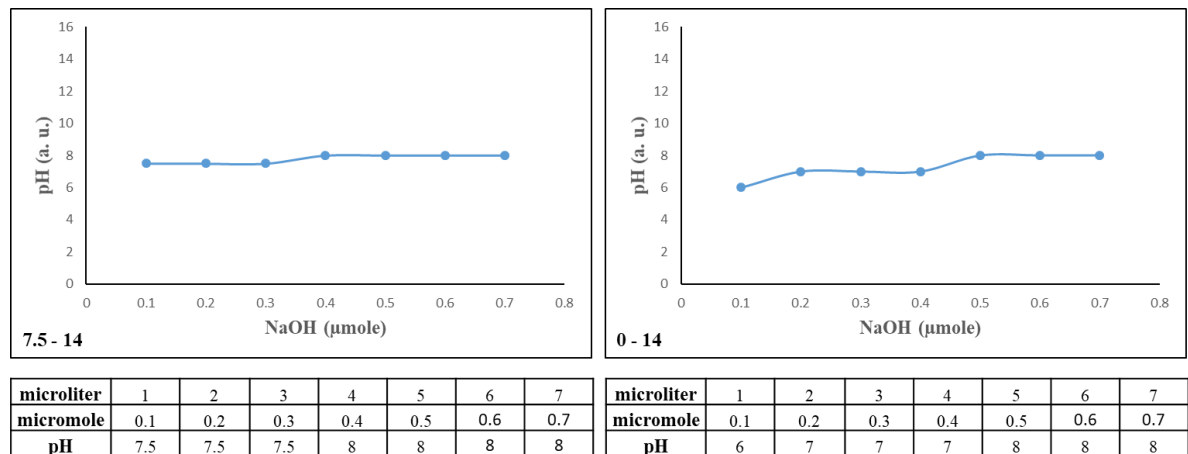


Figure 3.2. The tested amounts which are between 1 and 7  $\mu\text{l}$  were shown in table both in  $\mu\text{l}$  and  $\mu\text{mole}$  of NaOH values. At the same time, graphics were represented the exact pH value corresponding to the  $\mu\text{mole}$  value.

In collagen preparation protocol, NaOH amount which was calculated according to final concentration amount of collagen was 7.14 microliters in 100 microliter total collagen mixture. For this reason, samples in second groups were prepared based on this calculation and tested 4 different amounts of NaOH. These are 7.14 – 21.42 – 42.84 – 50 microliters, respectively. Each collagen samples were measured two different types of pH papers which were measure range value between 7.5 – 14 and 0 – 14. In this time, tested amounts were high, so pH values were shown broad ranges which were varied between 8 – 13 value (Figure 3.3.).

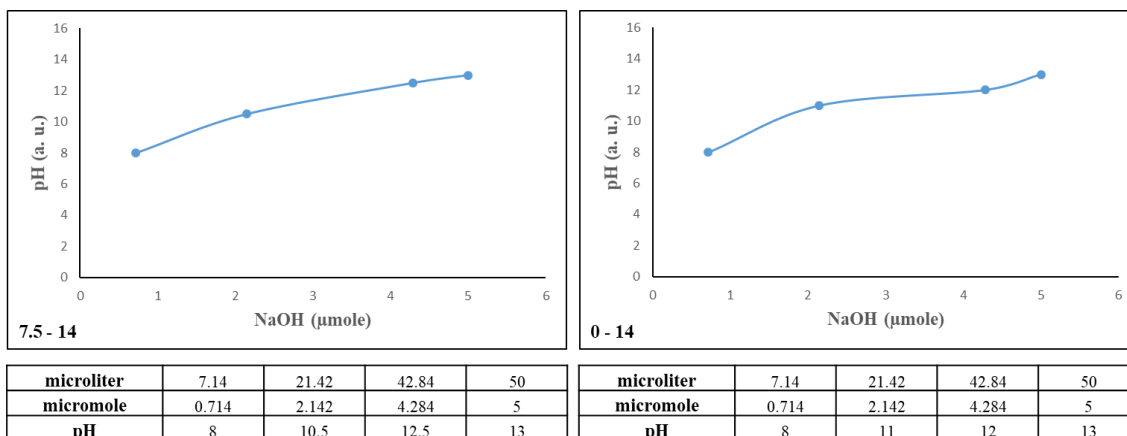


Figure 3.3. The tested amounts which are 7.14 – 21.42 – 42.84 – 50  $\mu\text{l}$  were shown in table both in  $\mu\text{l}$  and  $\mu\text{mole}$  of NaOH values. At the same time, graphics were represented the exact pH value corresponding to the  $\mu\text{mole}$  value.

In order to observe remaining values except the other ones, 3 different samples were prepared which were 20, 25 and 30 microliters, respectively. Each collagen samples were measured two different types of pH papers which were measure range value between 7.5 – 14 and 0 – 14. Difference between tested amounts of NaOH were not too much like second groups, for this reason changes of pH value was few as a first group result. This similarity was just in changing in pH value, so obtained quantitative results were different (Figure 3.4.).

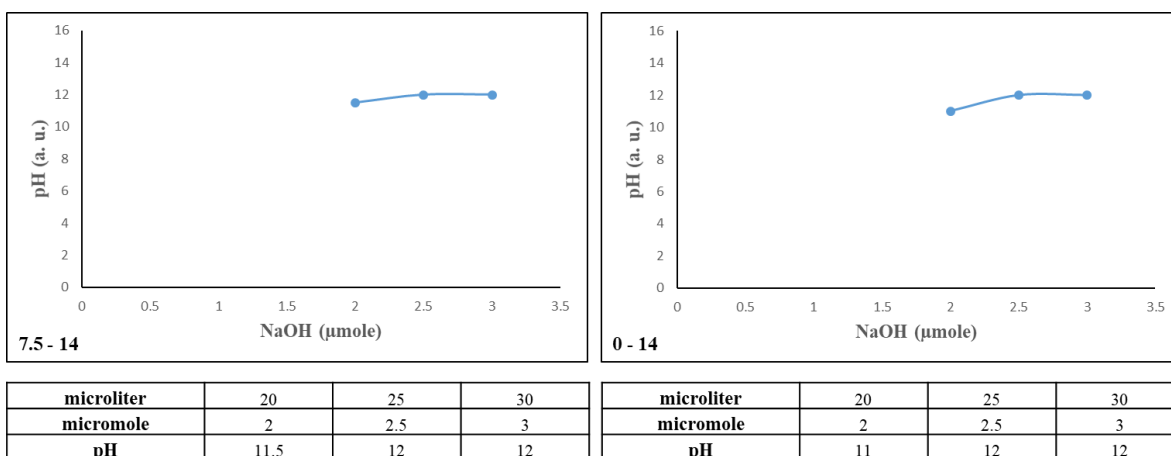


Figure 3.4. The tested amounts which are 20, 25 and 30  $\mu\text{l}$  were shown in table both in  $\mu\text{l}$  and  $\mu\text{mole}$  of NaOH values. At the same time, graphics were represented the exact pH value corresponding to the micromole value.

In order to observe the differences according to molarity value of NaOH (0.3M) amount, 5 different samples which were broad range value were prepared. Each collagen samples were measured two different types of pH papers which were measure range value between 7.5 – 14 and 0 – 14. Also, these groups were consisted different values which were tested in other groups. As a result, pH values were varied between 8 – 14 value (Figure 3.5.).

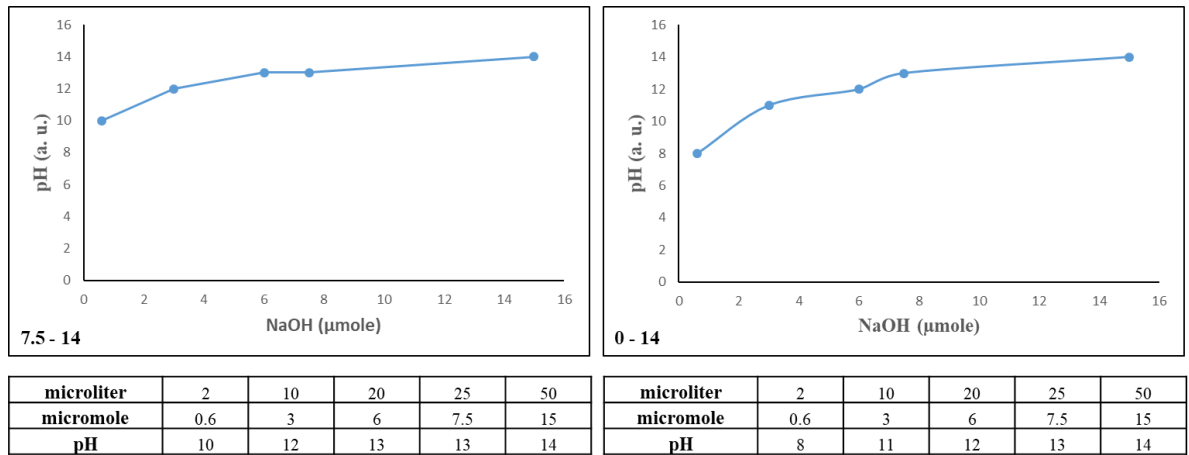


Figure 3.5. The tested amounts which are 2, 10, 20, 25 and 50  $\mu\text{l}$  at 0.3 M were shown in table both in  $\mu\text{l}$  and  $\mu\text{mole}$  of NaOH values. At the same time, graphics were represented the exact pH value corresponding to the  $\mu\text{mole}$  value.

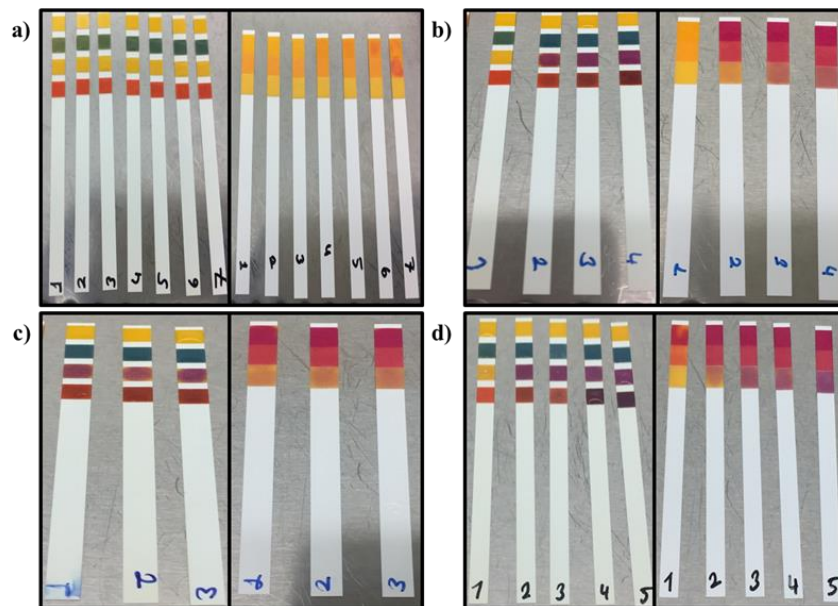


Figure 3.6. Measurement of Collagen pH according to different NaOH amount. a-c) 0.1 M NaOH, d) 0.3 M NaOH

As a result of evaluation of all experiments, two different pH values were decided to use, pH 7 and pH 12. Also, amount of NaOH was changed according to these values, 3 and 25 microliters, respectively. The important point here was to indicate the gel stiffness with appropriate both low and high pH value. Low pH and high pH values were represented soft gel and stiff gel, respectively. According to Yamamura et al. study relaxation modulus of collagen stiffness can be varying to pH of collagen solution. Differences between two values were kept high, so changing were observed easily. In these experiments stiffness of matrix condition was adjusted by pH dependent. Figure 3.7. shows sum-up of relation between NaOH amount in  $\mu\text{mole}$  value and their pH value.

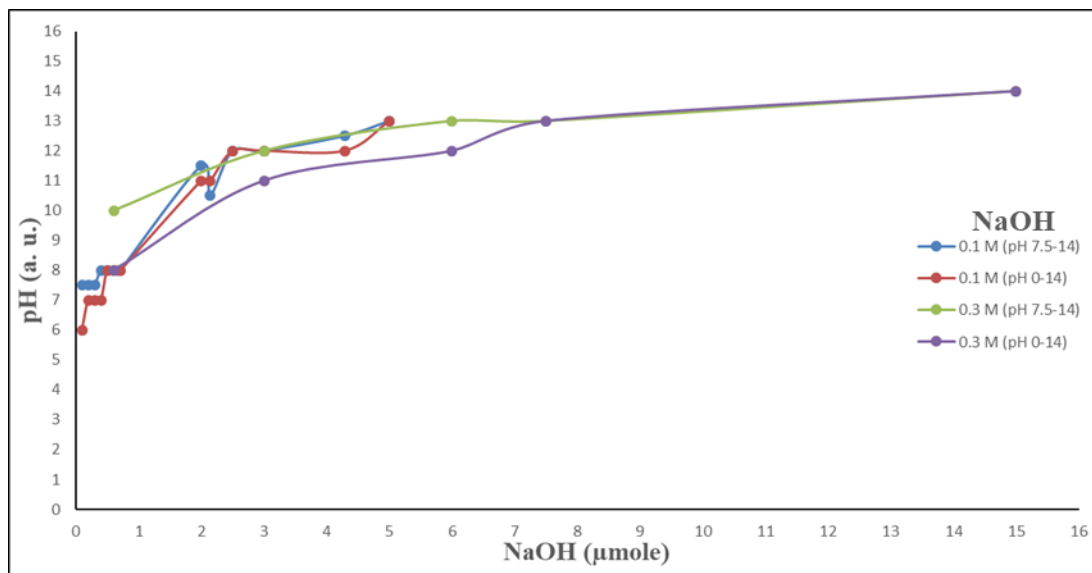


Figure 3.7. All tested amounts graphics were represented the exact pH value corresponding to the micromole value.

### 3.3. Coating Optimization of Lab-on-a-chip Device for the Formation of Endothelial Monolayer

Poly-L-lysine (PLL) is a type of poly amino acids which improves the cells attachments to surfaces. In the experiments, LOC devices were coated with PLL as a pre-coating protein and then FN was used as a second protein to provide an appropriate adherent surface for endothelial cells. When results were evaluated, endothelial cells which were used to mimic blood vessel increased their attachment to channel. Another

method was denoted by Asma Siddique et al. used 3-Aminopropyl triethoxysilane (APTES) in their study to create more appropriate microenvironment for cell growth. According to this study, APTES were used a linker between PDMS and collagen in surface coating<sup>84</sup>. This method was also applied by the combination of fibronectin. When we compare the results of different combination of coating materials (PLL-FN or APTES-FN), any significant differences were not observed in the terms of cell attachment. APTES is more advantageous for time cost according to PLL during coating process (Figure 3.8.).

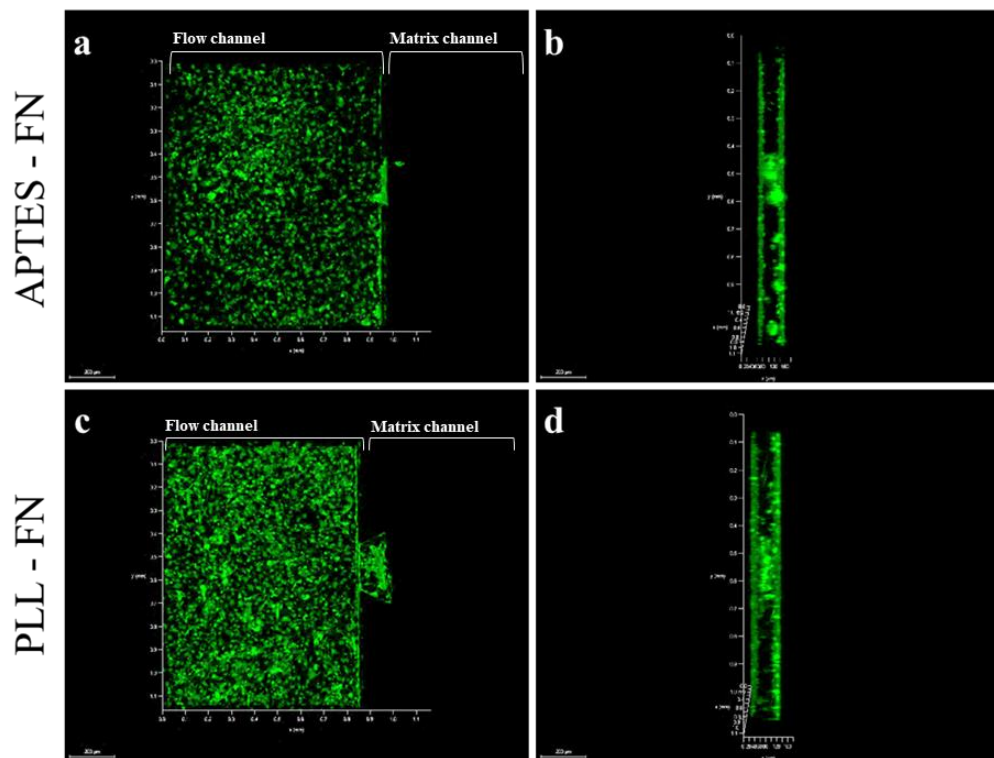


Figure 3.8. 3D microscope images of first day of 2% APTES-FN (0.0125 mg/ml) and 2% APTES-PLL (0.1 mg/ml) coated LOC devices with endothelial cells dissolved in dextran media. Images were taken with confocal microscope. a-b) Different positions of APTES – FN coated LOC devices. c-d) Different positions of PLL – FN coated LOC devices.

Other proteins such as laminin and collagen have also been tested as coating proteins in order to provide better adhesion of endothelial cells (bEnd.3) within LOC devices. When compared the different coating proteins effect on monolayer formation, some differences were observed. As a result of the experiment, the APTES-COL coating had some troubles for loading of endothelial cells into flow channel after coating process,

resulting in the leakage of other channels from flow channels during the loading process. The results showed that APTES-LAM (Figure 3.10.) were provided better surfaces for the generation of endothelial monolayer compare to APTES-FN (Figure 3.11.), APTES-COL (Figure 3.9.). APTES-LAM coating was used to mimic blood vessel in all extravasation experiments.

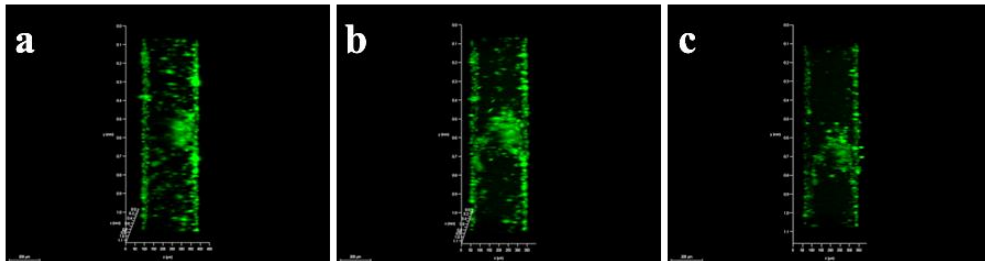


Figure 3.9. 3D microscope images were taken by confocal microscope of after bEnd.3 endothelial cells loading at a concentration  $7.5 \times 10^6$  / ml with 2% APTES - COL ( $5 \mu\text{g/ml}$ ) coated LOC device. a) first day, b) second day, c) third day.

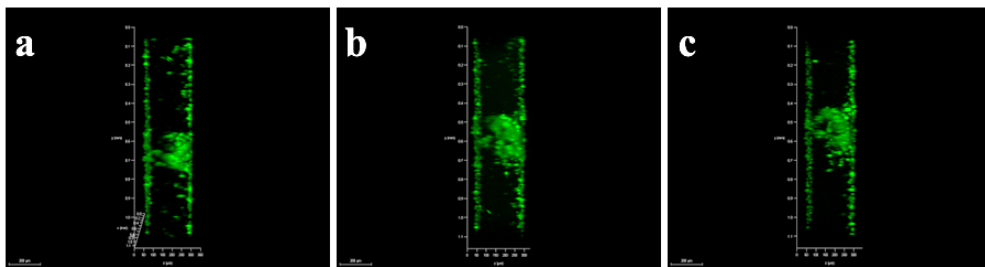


Figure 3.10. 3D microscope images were taken by confocal microscope of after bEnd.3 endothelial cells loading at a concentration  $7.5 \times 10^6$  / ml with 2% APTES - LAM ( $0.0125 \text{ mg/ml}$ ) coated LOC device. a) first day, b) second day, c) third day.

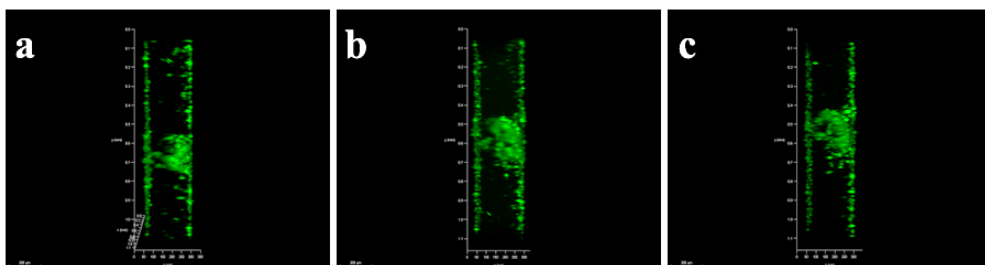


Figure 3.11. 3D microscope images were taken by confocal microscope of after bEnd.3 endothelial cells loading at a concentration  $7.5 \times 10^6$  / ml with 2% APTES - FN ( $0.0125 \text{ mg/ml}$ ) coated LOC device. a) first day, b) second day, c) third day.

### 3.4. Dextran used for Endothelial Monolayer

After overnight incubation, confocal photos were taken, but some partial aggregation and gaps between endothelial cells in channel were observed. According to Myers et al. study; dextran helps increasing of fluid viscosity, dependent on that velocity value of cell decreases<sup>85</sup>. So, cells adhere successfully on the surface. For this reason, endothelial cells were dissolved in both 8% dextran containing medium and normal bEnd.3 cells medium. When compared with dextran and no dextran samples, different results were obtained in endothelial cells coating. The results show that dextran allowed the endothelial cells disperse homogeneous in LOC devices. At the same time, endothelial cells with dissolved in dextran showed better adhesion and smooth coating between the posts of flow channel (Figure 3.12.).

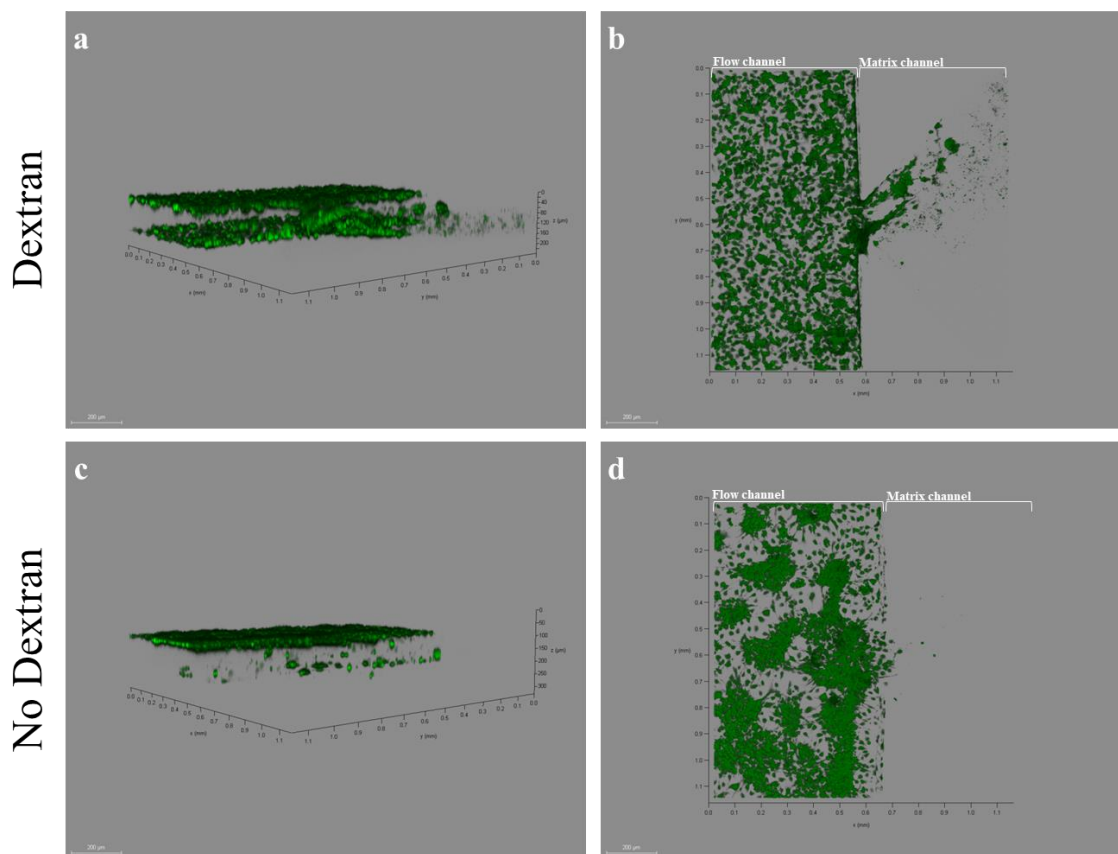


Figure 3.12. 3D microscope images of after bEnd.3 endothelial cells dissolved in dextran media and own media respectively loading at a concentration  $8.7 \times 10^6$  / ml with LOC device. a - c) Horizontal side view. b - d) Vertical side view.

### 3.5. Endothelial Monolayer Formation

In the endothelial monolayer experiments to be performed in LOC devices, it was the main objective to perform cells coating in the post region where the main extravasation was observed rather than the endothelial coating of the glass and PDMS surface. So, optimization of endothelial cell numbers has been tried at different concentrations depending on height of LOC devices. For all experiments, a mathematical calculation was made on how much cells should be loaded into the channel considering the average cell size and the area of the channel to be covered.

For this reason, the number of cells per microliter and the corresponding number of cells per micron were calculated. Starting from that, the most suitable concentration for endothelial cells monolayer coating was tested. In figure 3.7.;  $22 \times 10^4$ /ml endothelial cells were dissolved in  $150 \mu\text{l}$  dextran and loaded into LOC devices (Figure 3.13.). When the cell calculation was done for finding the number of cells per microliter,  $1466/\mu\text{l}$  bEnd.3 cell number was found. Each volume of flow channel of LOC devices was  $15 \mu\text{l}$ , so the required concentration of cells could be  $22 \times 10^3/15 \mu\text{l}$ . According to this calculation, it was decided that the number to be applied for the loading shall be  $30000 / 15\mu\text{l}$  for the next experiments, considering the whole of the post not being covered completely.

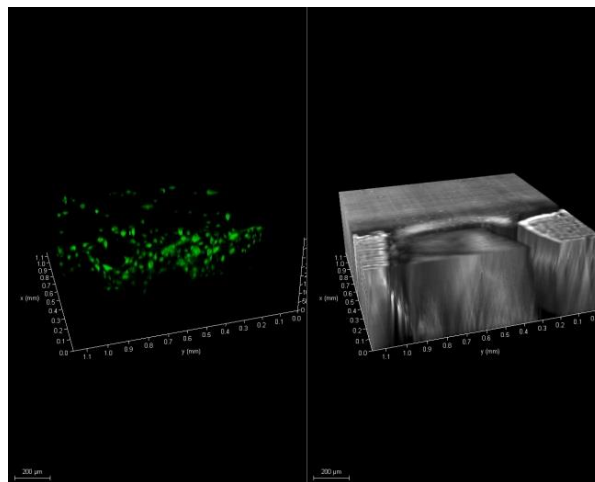


Figure 3.13. 3D microscope images of after bEnd.3 endothelial cells dissolved in dextran media loading at a concentration  $22 \times 10^4$  / ml with LOC device. a) Horizontal side view of green tracker labeled bEnd.3 cells. b) Horizontal side view of bright field.



This theoretically calculated value was tried on LOC devices which has 294 - micron height (Figure 3.14.).

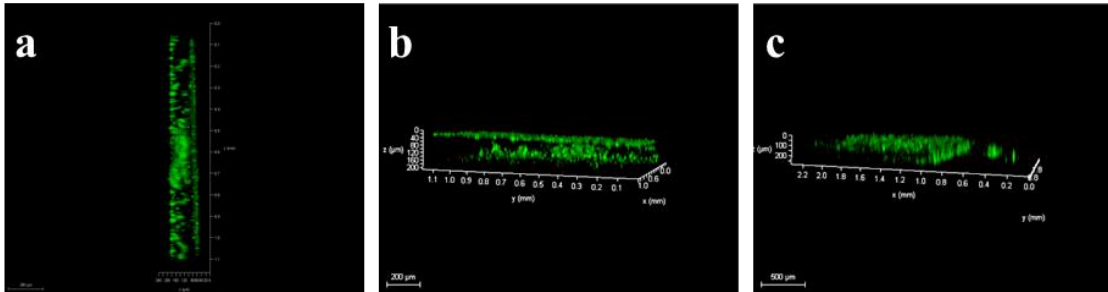


Figure 3.14. 3D microscope images were taken by confocal microscope of after bEnd.3 endothelial cells loading at a concentration  $5.8 \times 10^6$  / ml with 2% APTES – Laminin (0.0125 mg/ml) coated LOC device. a) Vertical side front of matrix channel view, b) Horizontal side behind of flow channel view, c) Horizontal side view.

At the end of experiments, monolayer which was formed by endothelial cells successfully. It was as a result of value calculated theoretically. According to these result, desired number of cells per micron was found to be 19736 cell / micron, so the optimization of cell number was completed.

Matrigel or Matrigel – Collagen mixtures were used as control groups during the optimization process. When the optimization step was completed successfully, following experiments were performed by using only collagen in different stiffness values. The results showed that the optimized number of cells were also applicable for only collagen matrix conditions (Figure 3.15. and Figure 3.16.).

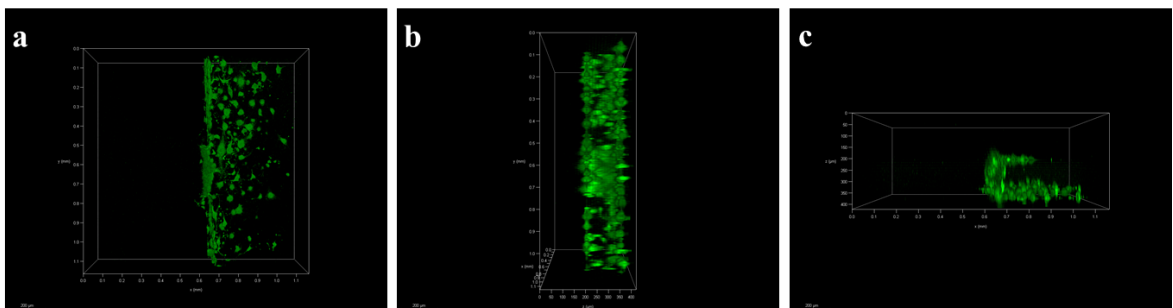


Figure 3.15. In matrix channel stiff collagen (high pH) was loaded. Then, 2% APTES – Laminin (0.0125 mg/ml) coated LOC device were loaded with bEnd.3 endothelial cells which was at a concentration  $5.2 \times 10^6$  / ml.

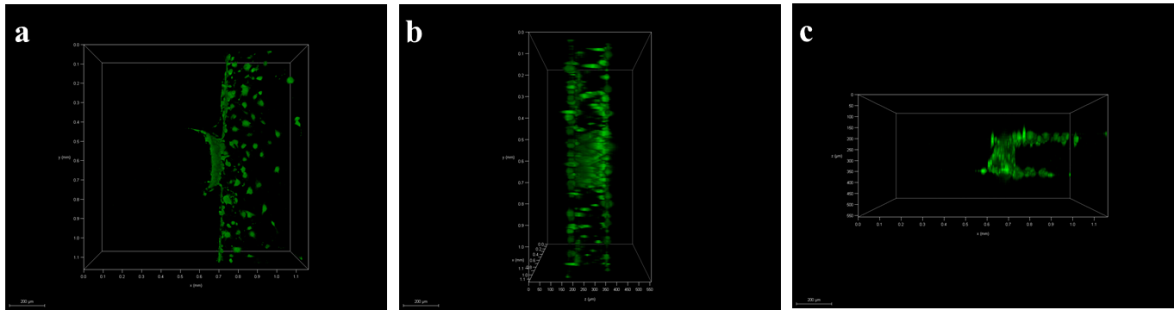


Figure 3.16. In matrix channel soft collagen (low pH) was loaded. Then 2% APTES – Laminin (0.0125 mg/ml) coated LOC device were loaded with bEnd.3 endothelial cells which was at a concentration  $5.2 \times 10^6$  / ml.

### 3.6. Determination of Permeability Differences

70 kDa dextran tetramethylrhodamine was applied to observe the endothelial monolayer integrity differences according to different stiffness of matrix (low pH and high pH conditions). In Figure 3.17. was shown differences between both low pH value (soft matrix) and high pH value (stiff matrix) in static conditions after loading the 70 kDa dextran. To compare the permeability effect, photos were taken in specific time interval (0 - 30 - 60 minutes). In low pH value (soft matrix) condition permeability was shown a few increasing. In contrast, in high pH value (soft matrix) condition permeability was increased faster when compare the low pH condition. When matrix structure has become stiffer, endothelial cell junctions are started to change. As a result of this, in high pH value matrix caused was caused of destabilization of endothelial cell junctions and promoted focal adhesion assembly. In addition, also changes in matrix structure were caused the increasing of permeability. In collagen structure fibril diameters and pore size were varied. When increased the pH value, fibril diameters are becoming shorter and pore sizes increased. That's why permeability was increased when using the high pH value condition. In addition, in Figure 3.18. graphics were showed the permeability differences between two matrix conditions during the specific time intervals. Blue bar was represented low pH, orange bar was represented high pH condition. During the 0- and 30- minutes time interval differences between two condition were not too much, but especially in 60 minutes differences were became higher.

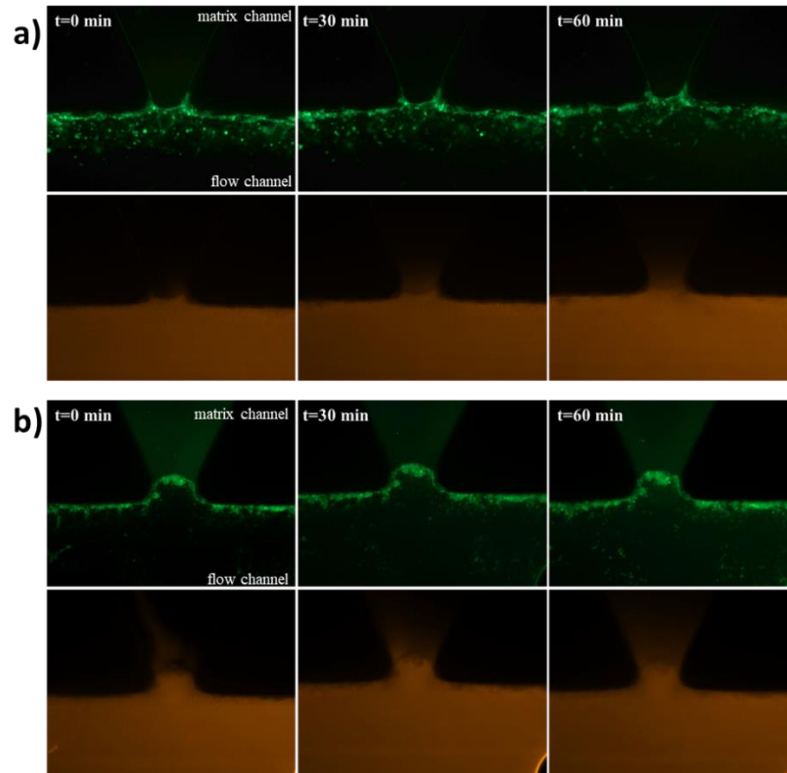


Figure 3.17. After 70kDa dextran loaded in flow channel. a) Low pH value collagen; top side bEnd.3 cells (488) 0-30-60 min. bottom side dextran (555). b) High pH value collagen; top side bEnd.3 cells (488) 0-30-60 min. bottom side dextran.

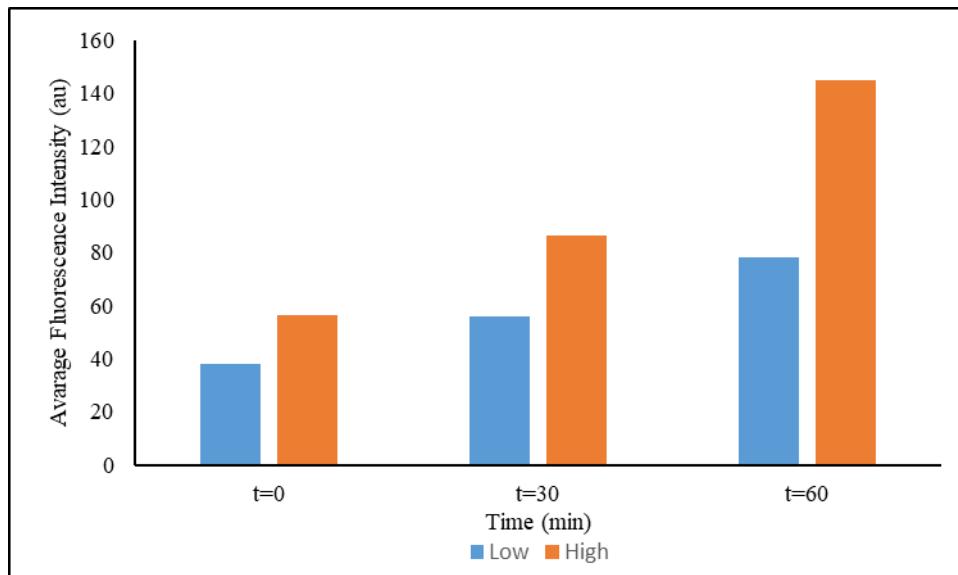


Figure 3.18. As a result of pH dependent collagen stiffness increased, cell-cell junction between endothelial cells were disrupted. For this reason, permeability is increased in high pH value of collagen.

### 3.7. Extravasated Cell Analysis

To comparison between extravasated MDA-MB-231 and MCF10A cells were analyzed according to cell number for both under static and flow condition in different stiffness value of collagen. Observation the relation between collagen stiffness and extravasation was shown in Figure 3.19. Significant difference was not observed when compared the extravasated cell number for MDA-MB-231 cells in both stiff (high pH) and soft (low pH) matrix conditions. However, flow and static conditions were also compared for the same matrix condition. In this comparison; significant differences were observed in extravasated cell number. For both soft and stiff matrix condition; decreasing of cell number was observed under the flow condition when compared the static condition ( $p < 0.05$  \*). Also, MCF10A cells both in soft and stiff matrix conditions were compared, there were no differences were observed. Moreover, MCF10A cells did not show significant differences even if in same matrix condition for both flow and static conditions. Lastly, MDA-MB-231 cells both in stiff - soft matrix and flow - static conditions groups were compared the MCF10A cells. MDA-MB-231 cells were indicated increasing significant differences when compared the MCF10A cells ( $p < 0.001$  \*\*\*).

In addition, these comprehensions associated cells also compared for both cell types, matrix conditions and flow - static conditions (Figure 3.21.). In static condition, significant differences were observed in MDA-MB-231 cells between the soft and stiff matrix conditions ( $p < 0.05$  \*). In soft matrix conditions associated cells numbers were higher than stiff matrix conditions for MDA-MB-231 cells. In contrast, MCF10 cells were shown significantly higher differences in stiff matrix conditions ( $p < 0.05$  \*). This situation may be caused different cell types. Also, cell types were compared in same matrix conditions. There were no significant differences in stiff matrix condition between MDA-MB-231 and MCF10A cells. However, MDA-MB-231 cells were increased significant differences when compared the MCF10A cells in soft matrix conditions ( $p < 0.05$  \*). When compared in flow conditions, there were no significant differences were observed even if both cell types and matrix conditions.

Lastly, cells which was found in flow channel were compared for both cell types, matrix conditions and flow - static conditions (Figure 3.22.). There were not any significant differences were observed between the all comprehension groups.

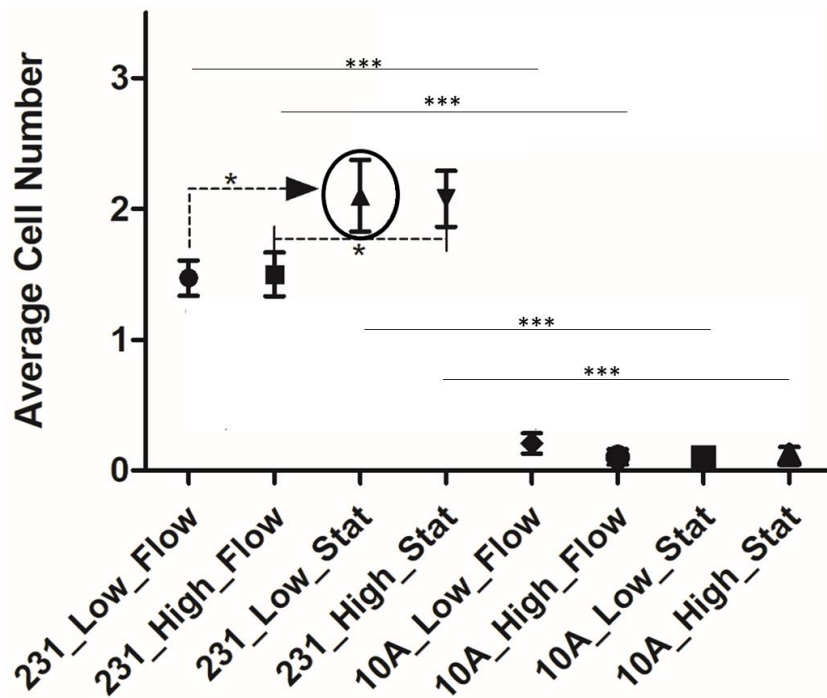


Figure 3.19. Extravasated cell number into matrix. Black line represents differences between MDA-MB-231 and MCF10A cells ( $p < 0.001$  \*\*\*), dashed lines represents differences between flow and static conditions of MDA-MB-231 cells in same matrix. ( $p < 0.05$  \*).

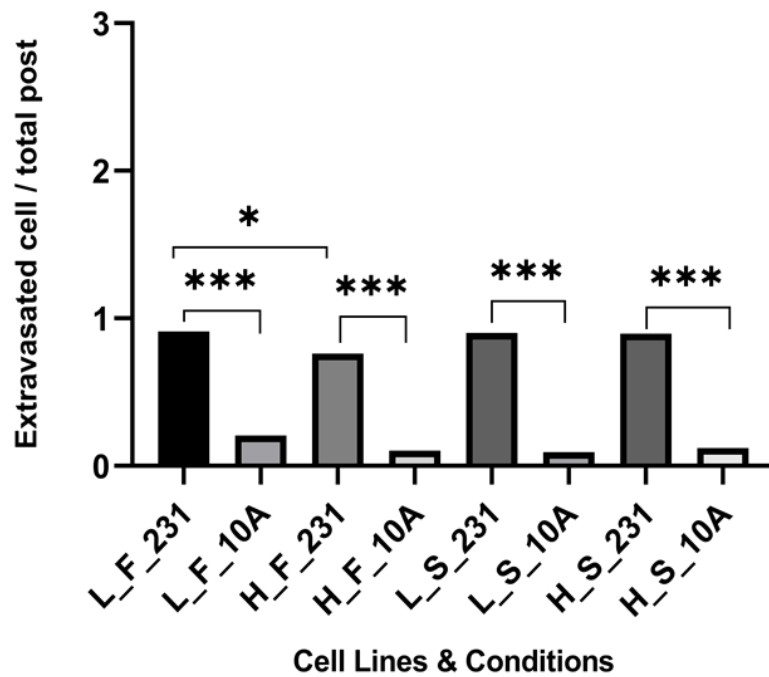


Figure 3.20. Extravasated cells metric in endothelial monolayer. ( $p < 0.05$  \*), ( $p < 0.001$  \*\*\*)

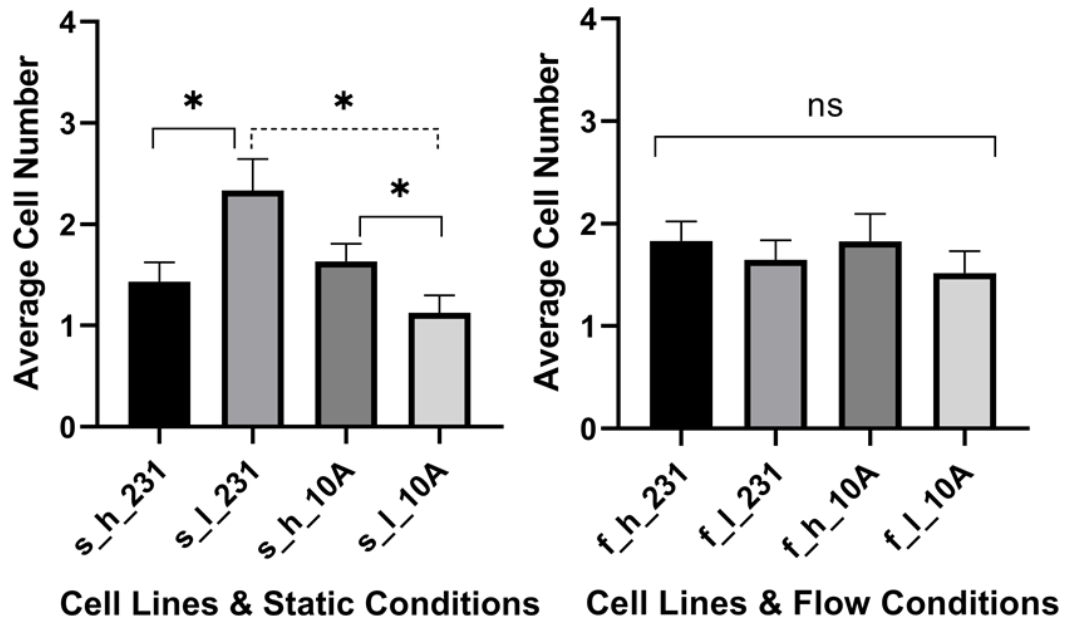


Figure 3.21. Associated cell number into matrix. Black line represents differences in MDA-MB-231 between soft and stiff matrix ( $p < 0.05$  \*), dashed lines represents differences between MDA-MB-231 and MCF10A cells in soft matrix under static condition. ( $p < 0.05$  \*).

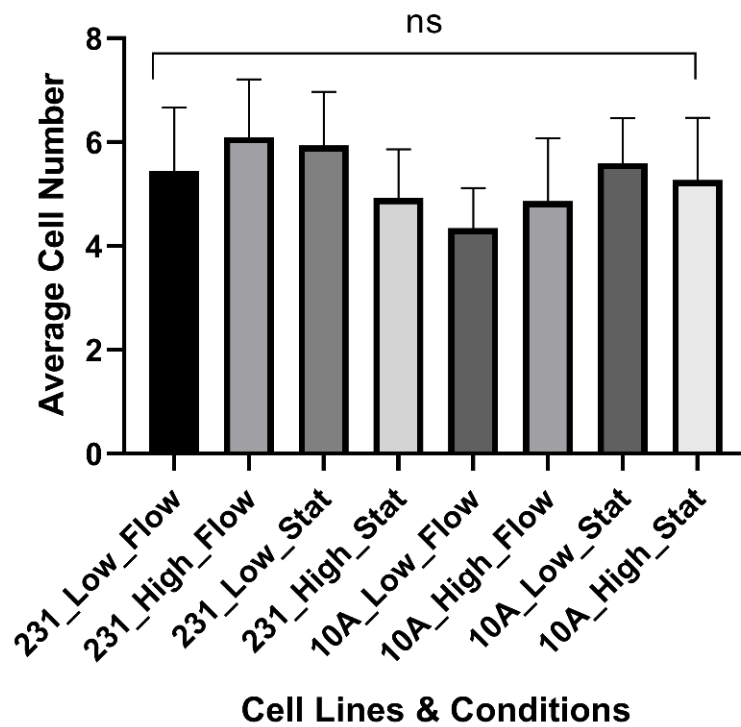


Figure 3.22. Cells number in flow channel.

### 3.8. Distance Migrated by Extravasated Cell

At the end of the cells extravasated, distance of cells across the endothelial monolayer must be calculated. This calculation may be used for the next step analysis. When comparing the distances of soft and stiff matrix for MDA-MB-231 cells in static conditions, it was significantly higher in stiff matrix than soft matrix ( $p < 0.01$  \*\*). Also, static conditions MDA-MB-231 in high matrix were shown increasing differences when compared to under-flow conditions. In contrast, when flow was applied in the same circumstances, there were no significant differences between matrix conditions (Figure 3.23.). In addition, MCF10A cells were not shown any significant differences when compared to soft and stiff matrix under static conditions. However, at flow conditions for MCF10A cells in stiff matrix were shown more distance when compared to soft matrix ( $p < 0.05$  \*). Thus, the flow may have triggered MCF10A cells (Figure 3.24.). Besides that, under constant matrix stiffness (stiff and soft) both MDA-MB-231 and MCF10 cells were compared under flow and static conditions. For both stiff and soft conditions separately, MDA-MB-231 cells were taken more distance as for that MCF10A cells (Figure 3.25. and Figure 3.26.).

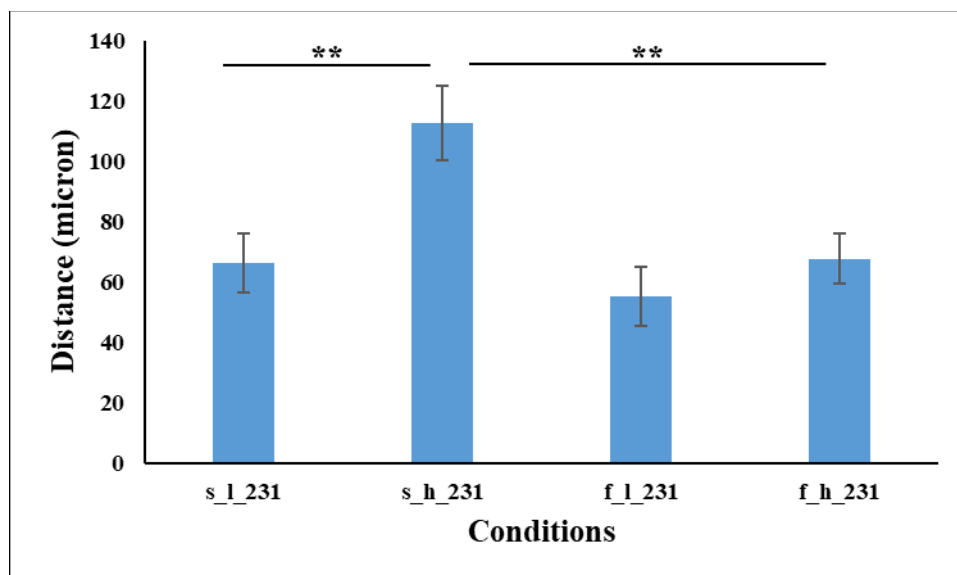


Figure 3.23. Distance of extravasated MDA-MB-231 cells both in stiff (high pH) and soft matrix (low pH) under flow and static conditions. ( $p < 0.01$  \*\*)

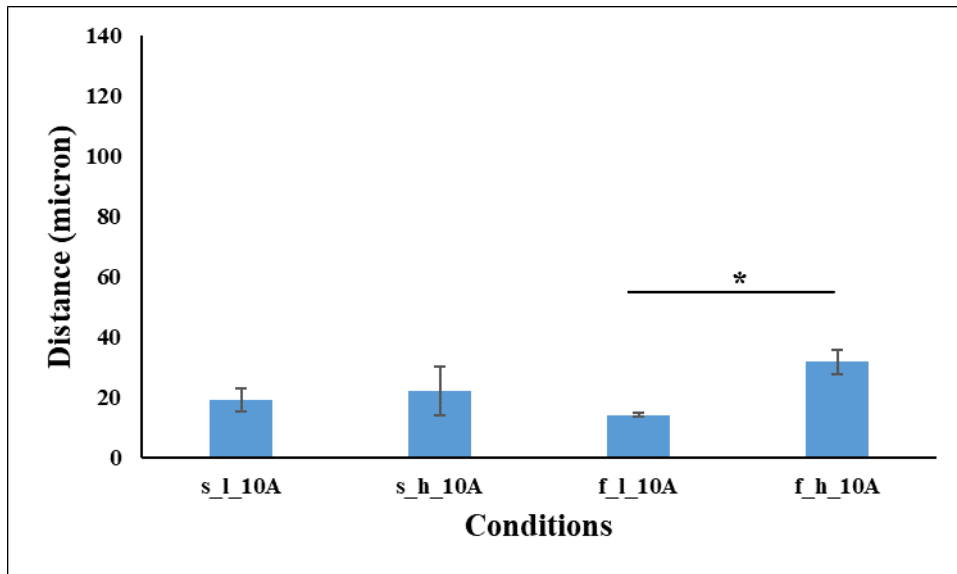


Figure 3.24. Distance of extravasated MCF10A cells both in stiff and soft matrix under flow and static condition. ( $p < 0.05$  \*)

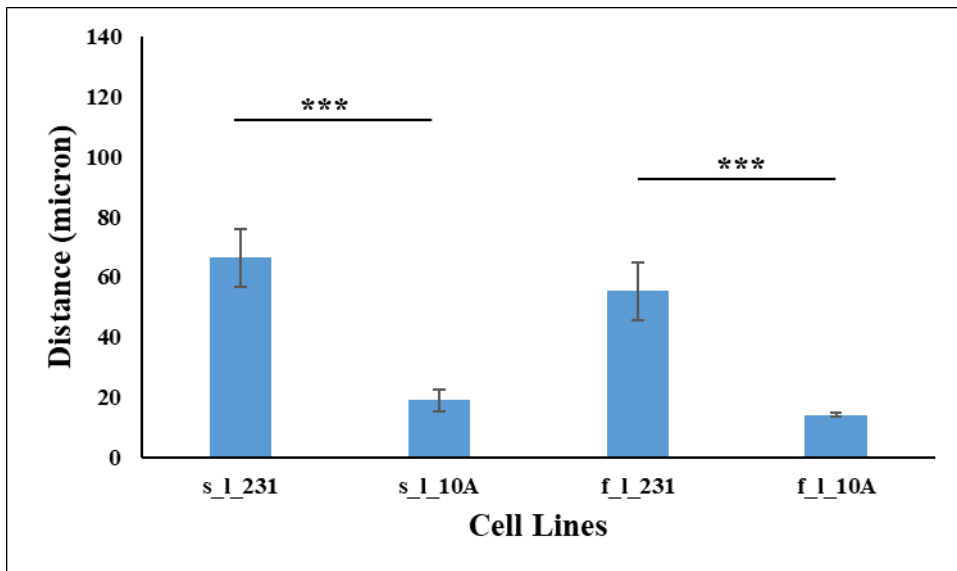


Figure 3.25. Comparison of distance of extravasated MDA-MB-231 and MCF10A cells in soft matrix under flow and static condition. ( $p < 0.001$  \*\*\*)



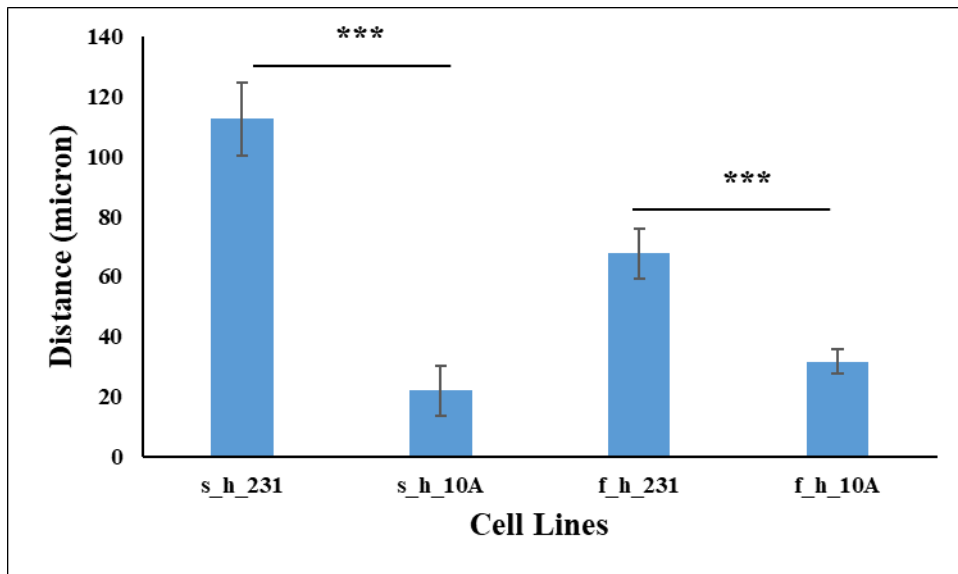


Figure 3.26. Comparison of distance of extravasated MDA-MB-231 and MCF10A cells in stiff matrix under flow and static condition. ( $p < 0.001$  \*\*\*)

## CHAPTER 4

### CONCLUSION

In this study, relation between extravasation which is the most significant step in cancer metastasis and extracellular matrix stiffness was investigated under both flow (perfusion) and static condition. LOC devices were used to as an in vitro model, so it was given to chance work on 3D microenvironment. In these devices; bEnd.3 cell line was used to form a blood vessel. To observe the extravasation effect; Invasive breast cancer cell line MDA-MB-231 and normal mammary epithelial cell line MCF10A were used.

In preparation steps of experiments, some optimizations were required on the purpose of providing appropriate environment to form of mimicking blood vessel in LOC devices. In coating method APTES and PLL were compared. APTES was selected coated material because of decreased the experiment time as against PLL. Also, other protein such as LAM, FN and COL were tried as a coating material for find a better cell adhesion to surface and LAM was selected for second coating material. Because of LAM was shown best adhesion results for endothelial cells monolayer. During the loading step of bEnd.3 endothelial cells, dextran was chosen as the ideal substrate for dissolving the cells when compared the own media. Because of their increasing the fluid viscosity features.

Coating of bEnd.3 as monolayer different cell numbers were tested to find the appropriate number. According to these result, different cell numbers were tried. As a result, desired number of cells per micron was found to be 19736 cell / micron.

Because of collagen was widely used in stiffness experiment, it was selected to mimic extracellular matrix in experiments. Collagen stiffness can change according to varying properties. In this study, pH dependent changes were applied to form different types collagen. Like Chung et al. study low pH value was represented soft matrix, in contrast high pH value was represented stiff matrix.

In high pH value (soft matrix) condition permeability was increased faster when compare the low pH condition. As a result of this, in high pH value matrix caused was caused of destabilization of endothelial cell junctions and promoted focal adhesion assembly. In addition that increasing the pH value, fibril diameters are becoming shorter

and pore sizes increased. That's why permeability was increased when using the high pH value condition

When compared the extravasated cell number between different stiffness matrix in same cell types, it was observed differences in quantitatively, but this result was not shown significant. However significant differences were observed when MDA-MB-231 cells evaluated separately both in soft and stiff matrix compared between flow and static conditions. So, cell numbers were decreased by applied flow. In addition, significant differences were observed between MDA-MB-231 and MCF10A cell lines in different matrix stiffness. Even if there are no significant differences between in different matrix condition, results were indicated that extravasation could be dependent on cell type and flow or static conditions. In contrast, matrix differences were affected both distances of two cell type. As a result, MDA-MB-231 cells in stiff matrix were tended to more go away when compare the soft matrix.

When compared the associated cell numbers, significantly differences were observed between soft and stiff matrix each cell types. Associated cells numbers were higher than stiff matrix conditions for MDA-MB-231 cells. In contrast, MCF10 cells were shown significantly higher differences in stiff matrix conditions. This situation may be caused different cell types. When compared in flow conditions, there were no significant differences were observed even if both cell types and matrix conditions. For cells which was found in flow channel were compared for both cell types, matrix conditions and flow - static conditions. No significant differences were observed between the all comprehension groups.

In addition, the use of microfluidic technologies has an importance to mimic in vivo conditions. Especially LOC devices useable to have many advantages. It is still unclear topic whether mechanical properties of different stiffness value of matrices underneath endothelial cells affect both MDA-MB-231 and MCF10A extravasation. According the results, relation between this question were tried to find.

## REFERENCES

1. Bray, F.; Ferlay, J.; Soerjomataram, I.; Siegel, R. L.; Torre, L. A.; Jemal, A., Global cancer statistics 2018: GLOBOCAN estimates of incidence and mortality worldwide for 36 cancers in 185 countries. *CA: a cancer journal for clinicians* **2018**, *68* (6), 394-424.
2. Langley, R. R.; Fidler, I. J., The seed and soil hypothesis revisited--the role of tumor-stroma interactions in metastasis to different organs. *International journal of cancer* **2011**, *128* (11), 2527-35.
3. Michor, F.; Iwasa, Y.; Nowak, M. A., Dynamics of cancer progression. *Nature Reviews Cancer* **2004**, *4* (3), 197-205.
4. Hanahan, D.; Weinberg, R. A., The hallmarks of cancer. *Cell* **2000**, *100* (1), 57-70.
5. Esmailsabzali, H.; Beischlag, T. V.; Cox, M. E.; Parameswaran, A. M.; Park, E. J., Detection and isolation of circulating tumor cells: principles and methods. *Biotechnology advances* **2013**, *31* (7), 1063-84.
6. Hanahan, D.; Weinberg, R. A., Hallmarks of cancer: the next generation. *Cell* **2011**, *144* (5), 646-74.
7. Hassiotou, F.; Geddes, D., Anatomy of the human mammary gland: Current status of knowledge. *Clinical anatomy (New York, N.Y.)* **2013**, *26* (1), 29-48.
8. Yoder, B. J.; Wilkinson, E. J.; Massoll, N. A., Molecular and morphologic distinctions between infiltrating ductal and lobular carcinoma of the breast. *The breast journal* **2007**, *13* (2), 172-9.
9. Lahart, I. M.; Metsios, G. S.; Nevill, A. M.; Carmichael, A. R., Physical activity, risk of death and recurrence in breast cancer survivors: A systematic review and meta-analysis of epidemiological studies. *Acta oncologica (Stockholm, Sweden)* **2015**, *54* (5), 635-54.
10. Nordqvist, C., What you need to know about breast cancer. Medical News Today, 2018.

11. Mansfield, C. M., A review of the etiology of breast cancer. *J Natl Med Assoc* **1993**, 85 (3), 217-221.
12. Esebua, M., Histopathology and grading of breast cancer. In *Cell and Molecular Biology of Breast Cancer*, Humana Press: 2013; pp 1-27.
13. McCready, T., Management of patients with breast cancer. *Nurs Stand* **2003**, 17 (41), 45-53; quiz 54, 56.
14. Cancer Facts & Figures 2018. American Cancer Society, 2018.
15. Dai, X.; Li, T.; Bai, Z.; Yang, Y.; Liu, X.; Zhan, J.; Shi, B., Breast cancer intrinsic subtype classification, clinical use and future trends. *American journal of cancer research* **2015**, 5 (10), 2929-43.
16. Weigelt, B.; Peterse, J. L.; van 't Veer, L. J., Breast cancer metastasis: markers and models. *Nature reviews. Cancer* **2005**, 5 (8), 591-602.
17. Urbano, R. L.; Furia, C.; Basehore, S.; Clyne, A. M., Stiff Substrates Increase Inflammation-Induced Endothelial Monolayer Tension and Permeability. *Biophysical journal* **2017**, 113 (3), 645-655.
18. Sporn, M. B., The War on Cancer: A Reviewa. *Annals of the New York Academy of Sciences* **1997**, 833 (1), 137-146.
19. Lambert, A. W.; Pattabiraman, D. R.; Weinberg, R. A., Emerging Biological Principles of Metastasis. *Cell* **2017**, 168 (4), 670-691.
20. Gupta, G. P.; Massagué, J., Cancer Metastasis: Building a Framework. *Cell* **2006**, 127 (4), 679-695.
21. Azevedo, A. S.; Follain, G.; Patthabhiraman, S.; Harlepp, S.; Goetz, J. G., Metastasis of circulating tumor cells: favorable soil or suitable biomechanics, or both? *Cell adhesion & migration* **2015**, 9 (5), 345-56.
22. Kai, F.; Laklai, H.; Weaver, V. M., Force Matters: Biomechanical Regulation of Cell Invasion and Migration in Disease. *Trends in cell biology* **2016**, 26 (7), 486-497.

23. Mierke, C. T., Cancer cells regulate biomechanical properties of human microvascular endothelial cells. *The Journal of biological chemistry* **2011**, 286 (46), 40025-37.
24. Stroka, K. M.; Konstantopoulos, K., Physical biology in cancer. 4. Physical cues guide tumor cell adhesion and migration. *American journal of physiology. Cell physiology* **2014**, 306 (2), C98-c109.
25. Riahi, R.; Yang, Y. L.; Kim, H.; Jiang, L.; Wong, P. K.; Zohar, Y., A microfluidic model for organ-specific extravasation of circulating tumor cells. *Biomicrofluidics* **2014**, 8 (2), 024103-024103.
26. Hamilla, S. M.; Stroka, K. M.; Aranda-Espinoza, H., VE-Cadherin-Independent Cancer Cell Incorporation into the Vascular Endothelium Precedes Transmigration. *PLOS ONE* **2014**, 9 (10), e109748.
27. Chambers, A. F.; Groom, A. C.; MacDonald, I. C., Dissemination and growth of cancer cells in metastatic sites. *Nature Reviews Cancer* **2002**, 2 (8), 563-572.
28. Thiery, J. P., Epithelial–mesenchymal transitions in tumour progression. *Nature Reviews Cancer* **2002**, 2 (6), 442-454.
29. Paget, S., THE DISTRIBUTION OF SECONDARY GROWTHS IN CANCER OF THE BREAST. *The Lancet* **1889**, 133 (3421), 571-573.
30. Wirtz, D.; Konstantopoulos, K.; Searson, P. C., The physics of cancer: the role of physical interactions and mechanical forces in metastasis. *Nature reviews. Cancer* **2011**, 11 (7), 512-22.
31. Gattazzo, F.; Urciuolo, A.; Bonaldo, P., Extracellular matrix: a dynamic microenvironment for stem cell niche. *Biochimica et biophysica acta* **2014**, 1840 (8), 2506-19.
32. Lampi, M. C.; Reinhart-King, C. A., Targeting extracellular matrix stiffness to attenuate disease: From molecular mechanisms to clinical trials. *Science translational medicine* **2018**, 10 (422).

33. Trappmann, B.; Chen, C. S., How cells sense extracellular matrix stiffness: a material's perspective. *Current opinion in biotechnology* **2013**, *24* (5), 948-53.
34. Egeblad, M.; Rasch, M. G.; Weaver, V. M., Dynamic interplay between the collagen scaffold and tumor evolution. *Current opinion in cell biology* **2010**, *22* (5), 697-706.
35. Hynes, R. O., The extracellular matrix: not just pretty fibrils. *Science* **2009**, *326* (5957), 1216-1219.
36. Huynh, J.; Nishimura, N.; Rana, K.; Peloquin, J. M.; Califano, J. P.; Montague, C. R.; King, M. R.; Schaffer, C. B.; Reinhart-King, C. A., Age-related intimal stiffening enhances endothelial permeability and leukocyte transmigration. *Science translational medicine* **2011**, *3* (112), 112ra122.
37. Adelow, C.; Segura, T.; Hubbell, J. A.; Frey, P., The effect of enzymatically degradable poly (ethylene glycol) hydrogels on smooth muscle cell phenotype. *Biomaterials* **2008**, *29* (3), 314-26.
38. Schmeichel, K. L.; Bissell, M. J., Modeling tissue-specific signaling and organ function in three dimensions. *Journal of cell science* **2003**, *116* (Pt 12), 2377-88.
39. Weigelt, B.; Ghajar, C. M.; Bissell, M. J., The need for complex 3D culture models to unravel novel pathways and identify accurate biomarkers in breast cancer. *Advanced drug delivery reviews* **2014**, *69-70*, 42-51.
40. Naba, A.; Clauser, K. R.; Whittaker, C. A.; Carr, S. A.; Tanabe, K. K.; Hynes, R. O., Extracellular matrix signatures of human primary metastatic colon cancers and their metastases to liver. *BMC Cancer* **2014**, *14* (1), 518.
41. Kharkar, P. M.; Kiick, K. L.; Kloxin, A. M., Designing degradable hydrogels for orthogonal control of cell microenvironments. *Chemical Society reviews* **2013**, *42* (17), 7335-72.

42. Pickup, M. W.; Mouw, J. K.; Weaver, V. M., The extracellular matrix modulates the hallmarks of cancer. *EMBO reports* **2014**, *15* (12), 1243-53.
43. Mehta, D.; Malik, A. B., Signaling mechanisms regulating endothelial permeability. *Physiological reviews* **2006**, *86* (1), 279-367.
44. Discher, D. E.; Janmey, P.; Wang, Y. L., Tissue cells feel and respond to the stiffness of their substrate. *Science* **2005**, *310* (5751), 1139-43.
45. Discher, D. E.; Mooney, D. J.; Zandstra, P. W., Growth factors, matrices, and forces combine and control stem cells. *Science* **2009**, *324* (5935), 1673-7.
46. Yeung, T.; Georges, P. C.; Flanagan, L. A.; Marg, B.; Ortiz, M.; Funaki, M.; Zahir, N.; Ming, W.; Weaver, V.; Janmey, P. A., Effects of substrate stiffness on cell morphology, cytoskeletal structure, and adhesion. *Cell motility and the cytoskeleton* **2005**, *60* (1), 24-34.
47. Krishnan, R.; Klumpers, D. D.; Park, C. Y.; Rajendran, K.; Trepap, X.; van Bezu, J.; van Hinsbergh, V. W.; Carman, C. V.; Brain, J. D.; Fredberg, J. J.; Butler, J. P.; van Nieuw Amerongen, G. P., Substrate stiffening promotes endothelial monolayer disruption through enhanced physical forces. *American journal of physiology. Cell physiology* **2011**, *300* (1), C146-54.
48. DuFort, C. C.; Paszek, M. J.; Weaver, V. M., Balancing forces: architectural control of mechanotransduction. *Nature reviews. Molecular cell biology* **2011**, *12* (5), 308-19.
49. Engler, A. J.; Sen, S.; Sweeney, H. L.; Discher, D. E., Matrix elasticity directs stem cell lineage specification. *Cell* **2006**, *126* (4), 677-89.
50. Kaess, B. M.; Rong, J.; Larson, M. G.; Hamburg, N. M.; Vita, J. A.; Levy, D.; Benjamin, E. J.; Vasan, R. S.; Mitchell, G. F., Aortic stiffness, blood pressure progression, and incident hypertension. *Jama* **2012**, *308* (9), 875-81.
51. Humphrey, J. D.; Dufresne, E. R.; Schwartz, M. A., Mechanotransduction and extracellular matrix homeostasis. *Nature reviews. Molecular cell biology* **2014**, *15* (12), 802-812.



52. Bonnans, C.; Chou, J.; Werb, Z., Remodelling the extracellular matrix in development and disease. *Nature reviews. Molecular cell biology* **2014**, *15* (12), 786-801.
53. Kohn, J. C.; Lampi, M. C.; Reinhart-King, C. A., Age-related vascular stiffening: causes and consequences. *Frontiers in genetics* **2015**, *6*, 112.
54. Fenner, J.; Stacer, A. C.; Winterroth, F.; Johnson, T. D.; Luker, K. E.; Luker, G. D., Macroscopic Stiffness of Breast Tumors Predicts Metastasis. *Scientific Reports* **2014**, *4*, 5512.
55. Alonso, J. L., Goldmann, W. H., Cellular mechanotransduction. *AIMS Biophysics* **2016**, 50-62.
56. Bershadsky, A. D.; Balaban, N. Q.; Geiger, B., Adhesion-dependent cell mechanosensitivity. *Annual review of cell and developmental biology* **2003**, *19*, 677-95.
57. Paszek, M. J.; Zahir, N.; Johnson, K. R.; Lakins, J. N.; Rozenberg, G. I.; Gefen, A.; Reinhart-King, C. A.; Margulies, S. S.; Dembo, M.; Boettiger, D.; Hammer, D. A.; Weaver, V. M., Tensional homeostasis and the malignant phenotype. *Cancer cell* **2005**, *8* (3), 241-54.
58. Chin, L.; Xia, Y.; Discher, D. E.; Janmey, P. A., Mechanotransduction in cancer. *Current opinion in chemical engineering* **2016**, *11*, 77-84.
59. Shi, Q.; Ghosh, R. P.; Engelke, H.; Rycroft, C. H.; Cassereau, L.; Sethian, J. A.; Weaver, V. M.; Liphardt, J. T., Rapid disorganization of mechanically interacting systems of mammary acini. *Proceedings of the National Academy of Sciences* **2014**, *111* (2), 658.
60. Kolahi, K. S.; Donjacour, A.; Liu, X.; Lin, W.; Simbulan, R. K.; Bloise, E.; Maltepe, E.; Rinaudo, P., Effect of Substrate Stiffness on Early Mouse Embryo Development. *PLOS ONE* **2012**, *7* (7), e41717.
61. Versaevel, M.; Grevesse, T.; Riaz, M.; Lantoine, J.; Gabriele, S., Micropatterning hydroxy-PAAm hydrogels and Sylgard 184 silicone elastomers with tunable elastic moduli. *Methods Cell Biol* **2014**, *121*, 33-48.

62. Skardal, A.; Mack, D.; Atala, A.; Soker, S., Substrate elasticity controls cell proliferation, surface marker expression and motile phenotype in amniotic fluid-derived stem cells. *Journal of the mechanical behavior of biomedical materials* **2013**, *17*, 307-16.
63. Doyle, A. D.; Yamada, K. M., Mechanosensing via cell-matrix adhesions in 3D microenvironments. *Experimental cell research* **2016**, *343* (1), 60-66.
64. Guiro, K.; Patel, S. A.; Greco, S. J.; Rameshwar, P.; Arinzeh, T. L., Investigating breast cancer cell behavior using tissue engineering scaffolds. *PloS one* **2015**, *10* (3), e0118724-e0118724.
65. Nelson, C. M.; Bissell, M. J., Modeling dynamic reciprocity: engineering three-dimensional culture models of breast architecture, function, and neoplastic transformation. *Seminars in cancer biology* **2005**, *15* (5), 342-52.
66. Rijal, G.; Li, W., 3D scaffolds in breast cancer research. *Biomaterials* **2016**, *81*, 135-156.
67. Levental, I.; Georges, P. C.; Janmey, P. A., Soft biological materials and their impact on cell function. *Soft Matter* **2007**, *3* (3), 299-306.
68. Schlunck, G.; Han, H.; Wecker, T.; Kampik, D.; Meyer-ter-Vehn, T.; Grehn, F., Substrate rigidity modulates cell matrix interactions and protein expression in human trabecular meshwork cells. *Investigative ophthalmology & visual science* **2008**, *49* (1), 262-9.
69. Raub, C. B.; Putnam, A. J.; Tromberg, B. J.; George, S. C., Predicting bulk mechanical properties of cellularized collagen gels using multiphoton microscopy. *Acta biomaterialia* **2010**, *6* (12), 4657-65.
70. Achilli, M.; Mantovani, D., Tailoring Mechanical Properties of Collagen-Based Scaffolds for Vascular Tissue Engineering: The Effects of pH, Temperature and Ionic Strength on Gelation. *Polymers* **2010**, *2* (4).
71. Chung, S.; Sudo, R.; Mack, P. J.; Wan, C. R.; Vickerman, V.; Kamm, R. D., Cell migration into scaffolds under co-culture conditions in a microfluidic platform. *Lab on a chip* **2009**, *9* (2), 269-75.

72. Yamamura, N.; Sudo, R.; Ikeda, M.; Tanishita, K., Effects of the mechanical properties of collagen gel on the in vitro formation of microvessel networks by endothelial cells. *Tissue engineering* **2007**, *13* (7), 1443-53.
73. Jeon, J. S.; Bersini, S.; Gilardi, M.; Dubini, G.; Charest, J. L.; Moretti, M.; Kamm, R. D., Human 3D vascularized organotypic microfluidic assays to study breast cancer cell extravasation. *Proceedings of the National Academy of Sciences of the United States of America* **2015**, *112* (1), 214-9.
74. Florczyk, S. J.; Wang, K.; Jana, S.; Wood, D. L.; Sytsma, S. K.; Sham, J.; Kievit, F. M.; Zhang, M., Porous chitosan-hyaluronic acid scaffolds as a mimic of glioblastoma microenvironment ECM. *Biomaterials* **2013**, *34* (38), 10143-50.
75. Bersini, S.; Jeon, J. S.; Dubini, G.; Arrigoni, C.; Chung, S.; Charest, J. L.; Moretti, M.; Kamm, R. D., A microfluidic 3D in vitro model for specificity of breast cancer metastasis to bone. *Biomaterials* **2014**, *35* (8), 2454-61.
76. Bischel, L. L.; Young, E. W.; Mader, B. R.; Beebe, D. J., Tubeless microfluidic angiogenesis assay with three-dimensional endothelial-lined microvessels. *Biomaterials* **2013**, *34* (5), 1471-7.
77. Zhang, W.; Choi, D. S.; Nguyen, Y. H.; Chang, J.; Qin, L., Studying Cancer Stem Cell Dynamics on PDMS Surfaces for Microfluidics Device Design. *Scientific Reports* **2013**, *3*, 2332.
78. Soscia, D.; Belle, A.; Fischer, N.; Enright, H.; Sales, A.; Osburn, J.; Bennett, W.; Mukerjee, E.; Kulp, K.; Pannu, S.; Wheeler, E., Controlled placement of multiple CNS cell populations to create complex neuronal cultures. *PLOS ONE* **2017**, *12* (11), e0188146.
79. Bersini, S.; Jeon, J. S.; Moretti, M.; Kamm, R. D., In vitro models of the metastatic cascade: from local invasion to extravasation. *Drug Discov Today* **2014**, *19* (6), 735-742.
80. Portillo-Lara, R.; Annabi, N., Microengineered cancer-on-a-chip platforms to study the metastatic microenvironment. *Lab on a chip* **2016**, *16* (21), 4063-4081.

81. Ozdil, B.; Onal, S.; Oruc, T.; Pesen Okvur, D., Fabrication of 3D Controlled in vitro Microenvironments. *MethodsX* **2014**, *1*, 60-66.
82. Morier, P.; Vollet, C.; Michel, P. E.; Reymond, F.; Rossier, J. S., Gravity-induced convective flow in microfluidic systems: electrochemical characterization and application to enzyme-linked immunosorbent assay tests. *Electrophoresis* **2004**, *25* (21-22), 3761-8.
83. Bruus, H., Analytical Navier Stokes solutions. In *Theoretical Microfluidics*, OUP Oxford: 2008; pp 19-38.
84. Siddique, A.; Meckel, T.; Stark, R. W.; Narayan, S., Improved cell adhesion under shear stress in PDMS microfluidic devices. *Colloids and surfaces. B, Biointerfaces* **2017**, *150*, 456-464.
85. Myers, D. R.; Sakurai, Y.; Tran, R.; Ahn, B.; Hardy, E. T.; Mannino, R.; Kita, A.; Tsai, M.; Lam, W. A., Endothelialized microfluidics for studying microvascular interactions in hematologic diseases. *Journal of visualized experiments : JoVE* **2012**, (64).